Norwegian University
of Life Sciences

Master's Thesis 2017 30 ECTS
Faculty of Environmental Sciences and Natural Resource Management

Cost optimization of distributed power generation in southern Norway, with focus on renewable hybrid system configurations.

Vegard Bøe
Renewable Energy

Preface

With the completion of this thesis, my five-year study in the Renewable Energy program at Norwegian University of Life Sciences is concluded. This period in my life have given me both social and professional experiences that most certainly will be a part of me in the life ahead.

I am grateful to Muyiwa Samuel Adaramola for introducing me to the concept of renewable hybrid energy systems. Your guidance, humor, and open door have been highly valuable in the work with this thesis, and during the study. Additionally, the financial support for using the simulation software in the thesis is appreciated. Thanks to Anna Kipping for contributing with modelling of load values used in this thesis, and for the positive response. I would also like to thank the scientific staff at the Renewable Energy-department for always being available for help and discussions, and for five interesting years.

Thank you to Noe Ganske Annet for the countless songs, confusing dances, companionship and good times. To my fellow students in class of 2017 – thanks for discussions, laughter and lunches.

Finally, I would like to thank my family for support, Guro Flaarønning for being who she is, and Frode Frydenlund for providing feedback on my thesis.

Ås, May 9, 2017

Vegard Bøe

Abstract

This thesis examines the levelized cost of energy for different grid-connected electrical system configurations, with focus on renewable hybrid configurations, situated in Ås, Norway. The analysis has been conducted with hourly data on the local energy resource basis, load demand from an average detached household, and grid power prices on both extraction and injection to the grid. Renewable technologies that have been considered are solar PV and wind turbine. The analysis has been performed in HOMER, and the optimal solutions for each system configuration have been presented. Furthermore, two scenarios for grid sellback rate have been examined; scenario A assumed a rate equal to 1kr/kWh, scenario B assumed rates equal to hourly elspot values throughout one year.

The main findings are:

- Grid-only was the optimal system configuration with a levelized cost of energy (LCOE) equal to 0,77kr/kWh.
- Optimal renewable hybrid configurations were equal in both scenarios, with 1kW solar PV and 5kW wind turbine, and levelized cost of energy equal to 1,85kr/kWh.
- When investment subsidy was included for all configurations in scenario A, the hybrid configuration with 10kW PV and 5kW wind turbine achieved the same LCOE of 1,80kr/kWh as the hybrid configuration with 1kW PV and 5kW wind turbine.
- At an 30% increase of resource basis for both solar and wind in scenario B, the hybrid configuration of 10kW PV and 5kW wind turbine achieved a lower LCOE than the configuration with 1kW PV and 5kW wind turbine.
- The combination of wind turbine and PV-array in Ås did provide power generation for a longer period annually, but the wind resource basis was not sufficient to make a hybrid renewable configuration economically viable.

Sammendrag

I denne oppgaven undersøkes energikostnaden for forskjellige nettilkoblede elektriske systemkonfigurasjoner, med fokus på fornybare hybridkonfigurasjoner, lokalisert i Ås. Analysen har blitt utført med timesdata på det lokale energiressursgrunnlaget, elektrisitetsbehov for en gjennomsnittlig husholdning, og strømpriser for både kjøp og salg til strømnettet. Fornybare teknologier som er vurdert er solcelle og vindturbin. Analysen er utført i HOMER, og de optimale energikostnadene for hver systemkonfigurasjon er presentert. To scenarier på salgspris av strøm har blitt undersøkt; Scenario A antok en fast pris lik 1 kr/kWh, scenario B antok timesverdier som følger elspotprisen igjennom ett år.

De viktigste funnene er:

- Strømnett uten lokal kraftproduksjon var den optimale systemkonfigurasjonen med en energikostnad (LCOE) på 0,77kr/kWh.
- Optimal fornybar hybridkonfigurasjon var lik i begge scenarier, med 1kWp PV og 5kW vindturbin, og en energikostnad på 1,85kr/kWh.
- Når investeringsstøtte ble inkludert for alle konfigurasjoner i scenario A, oppnådde hybridkonfigurasjonen med 10kW PV og 5kW vindturbin samme energikostnad på 1,80kr/kWh som hybridkonfigurasjonen med 1kWp PV og 5kW vindturbin.
- Ved en 30% økning av ressursgrunnlaget for både sol og vind i scenario B oppnådde hybridkonfigurasjonen med 10kW PV og 5kW vindturbin lavere energikostnad enn konfigurasjonen med 1kW PV og 5kW vindturbin.
- Kombinasjonen av vindturbin og PV-moduler i Ås medførte kraftproduksjon i en lengre periode årlig, men vindressursgrunnlaget var ikke tilstrekkelig til å gjøre en fornybar hybridkonfigurasjon lønnsom.

Table of Contents

List of abbreviations

LCOE	Levelized cost of energy
CRF	Capital recovery factor
NPC	Net present cost
PV	Photovoltaic
WT	Wind turbine
HRES	Hybrid renewable energy system
HOMER	Hybrid Optimization Model for Electric Renewables
NREL	National Renewable Energy Laboratory
US$	United states dollars
NOK	Norwegian kroners
kWh	Kilowatt hours
MWh	Megawatt hours
GHG	Greenhouse gases
STC	Standard test conditions
NOCT	Normal operating cell temperature
DG	Distributed generation
kWp	Kilowatt peak
Wp	Watt peak
Cp	Capacity factor
El	Electricity
NVES	Norwegian Wind Energy Center
VAT	Value added tax (25%)
NPV	Net present value

1 Introduction

The consumption of fossil energy resources have proven to impose a considerable negative externality, and the implications for the utilization of energy resources in the world are tremendous. Fossil resources accounted for 66,7% of the global electricity generated in 2014, a number illustrating the significant role it plays in the global electricity mix (International Energy Agency 2016). Satisfying the demand for energy services must be done without degradation of the environment on both short and long term, and this constraint entail utilization of fossil resources to be reduced.

Norway is a nation with a large abundance of energy resources, where the two most prominent ones are fossil fuels (mostly, natural gas and crude oil) and water. Fossil fuels are mainly exported to other countries in Europe, while the water is converted into electricity in the numerous hydro power plants located across the country. Regulated hydropower are an essential part of the Norwegian electricity mix, accounted for 96% of the total electricity generation in 2015 (Holstad et al. 2016). As a renewable energy technology, regulated hydropower holds two essential characteristics; low GHG-emissions from production, and the possibility of regulating the amount of electricity generated. However, the physical impact from building regulated hydropower are substantial, and the number of rivers that can be regulated are limited.

Sweden and Norway are cooperating in the green certificate scheme with the objective of increasing electricity generation from renewable energy resources. In recent years, utilization of solar and wind resources have received increased attention from both power companies, politicians and the public in Norway. Costs for the two technologies have been declining, and the green certificates have made a number of wind energy projects profitable in Norway and Sweden (Kost et al. 2013). Although, the attention has been focused on different energy sources, there are a new perspective on development of the power system.

Power systems are traditionally arranged with central power plants transporting its generated electricity to locations where there are demand for power.

Transportation of power is made possible by transmission lines constructed at different scales, either above or under the ground. This way of arranging the power system have proven to be reliable, and have been assumed to be the most cost efficient for the society (Pérez-Arriaga et al. 2016 p.21). Yet, transporting electricity in power lines involve electrical losses, building power lines are highly capital intensive, the location of energy resources may be a great distance from where the power is consumed, and structures enabling generation and transportation are often located in areas with conflicting interests concerning environmental and cultural values. Therefore, distributed power generation are considered as one possible alternative to meeting demand for energy services.

Distributed power generation, in comparison with centralized power generation systems, are characterized by lower installed capacities and shorter transportation distance from generation site to consumption site. It can be grid-connected or standalone, and it can utilize site specific energy resources or energy carriers that are transported and converted into electricity at the site of consumption (Akinyele et al. 2014; Koussa & Koussa 2015).

The research on distributed power generation are increasing, where the main focus has been on standalone systems supplying a defined load. These kinds of systems are particularly interesting in areas where the entities consuming electricity is not connected to an electric distribution grid (Deshmukh & Deshmukh 2008). Furthermore, focus on abatement of greenhouse gas emissions and decreased dependence on fossil fuels have directed awareness towards utilization of renewable energy sources (Deshmukh & Deshmukh 2008). However, renewable energy sources, like wind and solar radiation, are intermittent and not possible to control without storage technologies, imposing the need for using base load technologies like diesel and gas generators (Sreeraj et al. 2010).

Systems utilizing only one renewable energy source, will not generate electricity at times when the available resources are insufficient, and load demand are generally not synchronized with the availability of resources (Adaramola et al. 2014; Mahesh & Sandhu 2015). Moreover, single-source systems are often over-

dimensioned and highly dependent on fossil fuels, which in return increase the life cycle cost and emissions. However, when multiple renewable sources are utilized in the same system, it becomes more robust in the ability to meet demand, the total cost of the system decreases, and base load reduces its time in operation. Which types of hybrid systems that are suitable for a specific location depends on the locally available energy resources (Bernal-Agustín & Dufo-López 2009; Deshmukh & Deshmukh 2008).

Research conducted on distributed hybrid electrical systems in Norway are scarce. Sarker (2016) examined the optimal energy system for a single standalone house located at Grimstad in Norway. The optimal system with lowest net present cost of US$72232, consisted of PV array, wind turbine, producer gas generator and battery. Levelized cost for this system was estimated at US$0,306/kWh (or NOK 2,632/kWh), significantly higher than the average grid power price of NOK 0,85/kWh based on the years 2012 to 2016 (Aanensen & Olaisen 2016). The author of this thesis has not succeeded in finding other articles on this matter. Furthermore, the majority of dwellings in Norway are connected to the grid, indicating that standalone systems are less relevant as long as the grid power price is lower than what standalone systems can deliver.

However, the interest in distributed generation have increased in Norway, where the main focus has been on installation of solar PV (Ramsdal 2017). Accumulated solar PV capacity have increased from 10,6MWp in 2013 to 26,7MWp in 2016, where 95% of the increase are in grid-connected systems (*Statistikk: Bruk av* 2017).

The question that came to my attention is how profitable grid-connected distributed electrical systems in Norway are, and how the performance and cost would be if hybrid configurations of PV and wind turbine was considered. ON this basis, an economic optimization assessment of a grid-connected distributed hybrid electrical system situated in Ås was decided to be the purpose of my thesis.

The objective of this thesis is divided into three:

1. Is distributed electricity generation, utilizing local solar and wind resources, profitable for an average household in Ås?
2. How does hybrid renewable electric system configurations compare to single renewable electric system configurations when considering levelized cost of energy?
3. What factors are most important in determining the levelized cost of energy for the hybrid system configurations?

As technologies develops, new possibilities in meeting energy demand arise. Innovative solutions to old problems can facilitate more effective resource utilization. The Norwegian power system meet its requirement successfully, delivering electricity to consumers in need at nearly all times (Hansen et al. 2017). However, distributed power generation may be a valuable addition to a centralized power system. Because consumers of electricity currently are the main installers of distributed electricity technologies, this thesis aims to assess the profitability for these stakeholders. Findings are aimed to contribute into the discussion on how electricity demand should be met in Norway. Furthermore, there is a gap in knowledge on economic performance of grid-connected hybrid electricity systems in northern climates. This thesis can hopefully be used to reduce a part of this gap, and as a reference to others who wish to examine the possibilities of distributed power generation.

2 Methodology

2.1 Load

Load profile is essential for designing a system possible of meeting the requirements for an entity consuming electricity. The analysis conducted in this thesis is sought to be made for an average household in Ås. Consumption of electricity in households depends on many factors, such as outdoor temperature, number of residents, and time of day. To capture the variability of load, the values provided are in hourly timesteps. However, the availability of measured representative hourly load data for households in Ås was not possible to obtain. Smart electricity meters, providing load measurements in timesteps smaller than one hour, are not installed before 2018 in Ås. As a result, modelled load values are used.

Hourly load values originate from the results of a model developed by Kipping and Trømborg (2016). The model has been developed based on hourly smart meter data, retrieved from customers at two power grid operators in Norway; Ringerikskraft Nett and Skagerak Nett AS. From this data, key variables necessary for modelling hourly electricity consumption have been determined.

Modelling of the load profile has been conducted exogenously of HOMER by Anna Kipping, and the assumptions have been made by her. Assumptions are presented in Table 2-1 (Kipping 2017a; Kipping 2017b). The modelled values are based on temperature readings in 2016 from Ås, weather station number 17850 (Kipping 2017c).

Table 2-1: Assumptions made when modelling the hourly load profile provided in HOMER.

Variable type	Value
Dwelling type	Detached house
Number of residents	2 adults, 2 children
Floor space	150 m²
Building build year	<1980
Heating source	Electricity (100%)

It is important to note that the modelled values for electricity consumption during June, July and August are more uncertain than the other months, because of limited data available when the model was created. Furthermore, consumption from electric vehicles have not been implemented in the model, which can have a significant impact. Finally, the load values must be interpreted as general average values, meaning that the load profiles for individual households may be significantly different than the ones provided here.

For the reference of the reader, monthly averages and extreme values are presented in Figure 2-1. The average daily load curve for each month is presented in Figure 2-2. Note that the figures only are visual presentation of the hourly values, while HOMER use hourly values in the simulations.

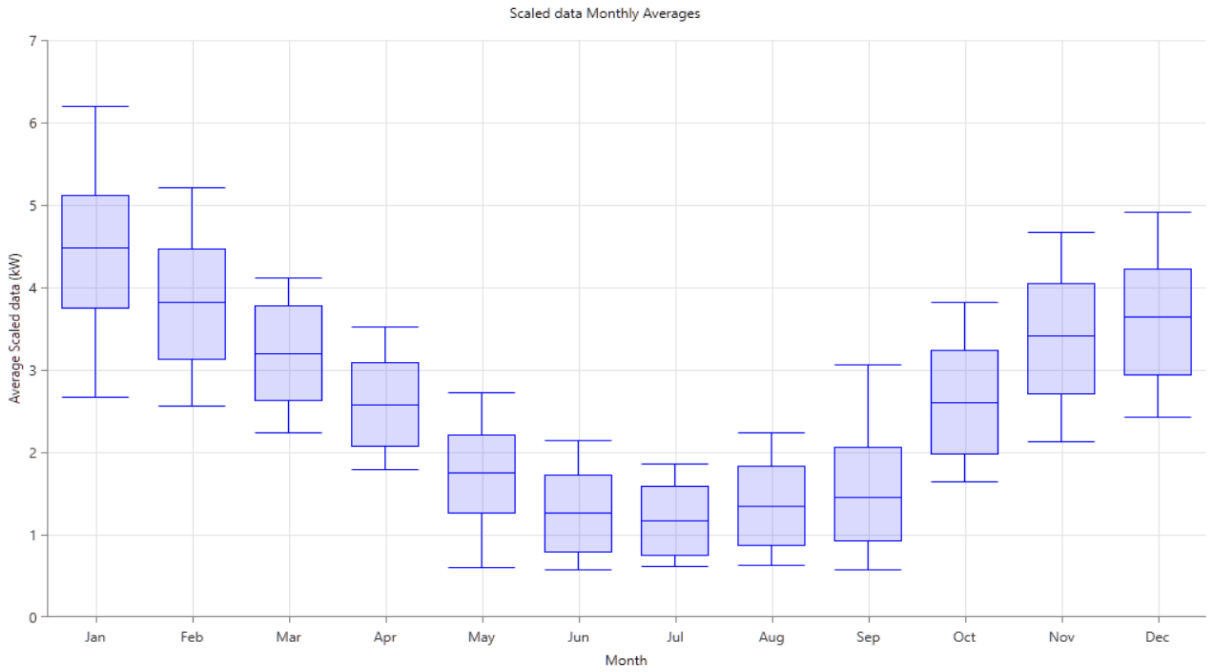

Figure 2-1: Monthly load values created from the load input values. The line at the top and bottom show the monthly maximum and minimum values respectively. The line at the top and bottom of the blue box show the average daily maximum and minimum value. The middle line show the average monthly load. Based on modelled load values.

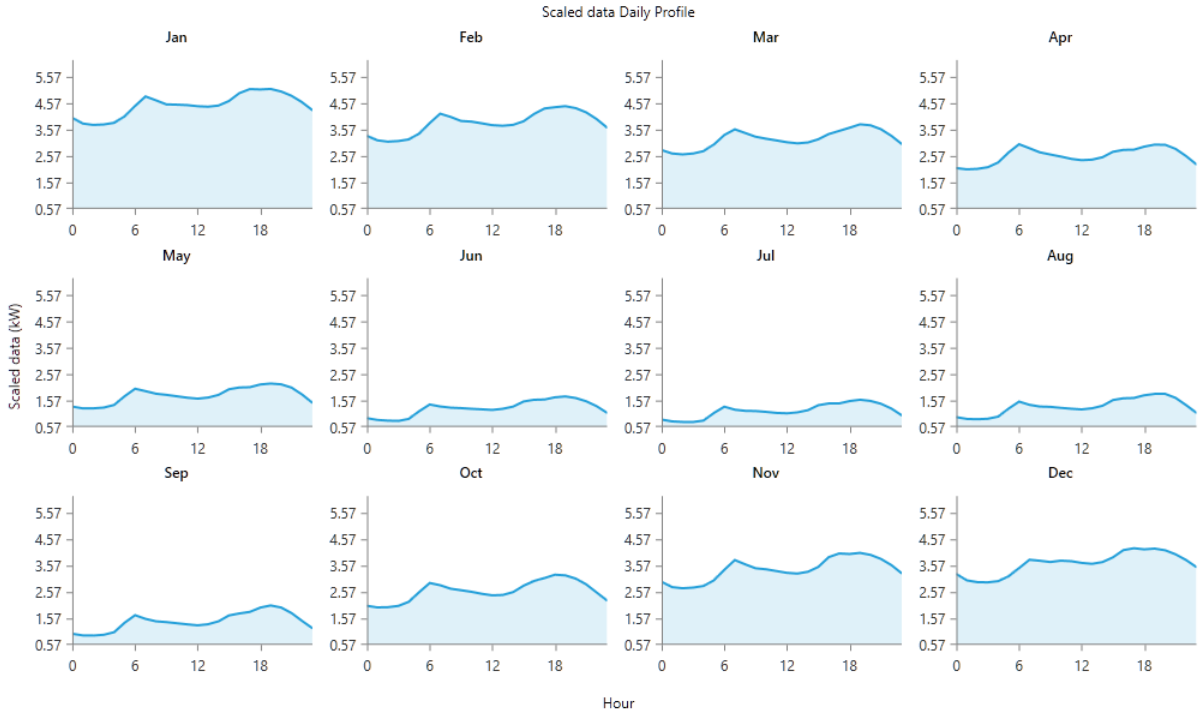

Figure 2-2: Average daily load profile for each month. The area under each curve show the daily average electricity demand in each month. Based on modelled load values.

Scaled annual daily average electricity consumption is 61,49kWh/day. Annual maximum-, minimum-, and average load is equal to 6,2kW, 0,5kW, and 2,56kW respectively. The load factor is 41%. No sensitivity variables have been assigned.

Two load variability values are calculated from the input data provided, named "Day-to-day" and "Timestep"-variability. These are useful if HOMER is used to generate a synthetic load profile that must be adapted to achieve a realistic load profile for a current project. Day-to-day variability indicate how much the load varies between each day. The load profile shape is retained, but the profile height is randomly varied between each day according to the day-to-day value. Timestep variability indicates the change in load between each timestep. The load profile shape are changed randomly according to the timestep value (Homer Energy 2016 p.253-256). Day-to-day variability is 12,648%, and timestep variability is 5,607%.

2.2 Renewable resources

The resource data used originate from the meteorological station named BIOKLIM, situated in Ås. It is located on Sørås, and operated by a group of scientists at the Norwegian University of Life Sciences (NMBU). The station is at a latitude of 59° 39' 37" N and a longitude of 10° 46' 54" E, 93,3 meters above sea level (*Om FAGKLIM* 2017). All meteorological input data are hourly averages from January 2006 to December 2016, provided by Kroken (2017). The data consists of global solar irradiance, wind speed and temperature. Eleven data points for each hour have been summarized into an arithmetically mean. The years 2008, 2012 and 2016 are leap years, resulting in values from 29. February in the mentioned years have been removed to achieve 8760 timesteps in each year. Note that all figures present monthly values of the available resources, while HOMER use hourly values in the simulations.

2.2.1 Solar radiation data

Solar energy can be utilized as an energy carrier in both thermal and electrical form. In this thesis, the potential for converting solar radiation into electricity will be examined. There are two main metrics that are used for measuring solar radiation; irradiance and irradiation.

Irradiance is given in W/m^2, and can be understood as the power falling on a specific area at any given time (Messenger & Ventre 2005 p.25). Irradiation is given in kWh/m^2, and is the energy density of sunlight that hits a specific area in a specified amount of time. Energy is defined as the integral of power over time, which in solar energy terms means that irradiation is the integral of irradiance. Irradiation is usually given per day, and the resulting unit is therefore $kWh/m^2/day$ (Messenger & Ventre 2005 p.25).

There are two types of solar radiation that are measured and used in determining the solar resource basis on a horizontal surface; direct and indirect radiation. Direct radiation is solar radiation that are received on a surface from the sun without being scattered by the atmosphere. Indirect radiation is

radiation received on a surface from the sun after its direction have been changed by the atmosphere. When the two types of radiation are summarized, they result in global radiation, which are the values used in the modelling (Duffie & Beckman 2013 p.10). The expression for total radiation on a horizontal surface are shown in Equation 1, and visualized in Figure 2-4.

$$\bar{G} = \bar{G}_d + \bar{G}_{id} \quad (1)$$

Where:

$\bar{G}_d$ is direct irradiance [kW/m^2]

$\bar{G}_{id}$ is indirect irradiance [kW/m^2]

Clearness index is a measure of the clearness in the atmosphere, indicating the fraction of radiation on top of the atmosphere hitting the earth. The value is high in periods with sunny conditions, and low at cloudy conditions, and can be calculated by using Equation 2 (Homer Energy 2016 p.225-227 and 333):

$$K_T = \frac{H_{ave}}{H_{0,ave}} \quad (2)$$

Where:

K_T is the clearness index in month T.

H_{ave} is the monthly average irradiance on the surface of the earth [kWh/m^2/day].

$H_{0,ave}$ is the irradiance on a horizontal surface on the top of the earth's atmosphere, also known as the extraterrestrial radiation [kWh/m^2/day].

Since global irradiation is the only data that are provided into the model, the clearness index is used to calculate the amount of indirect irradiation that strikes the tilted solar array (Homer Energy 2016 p.237-238). Monthly values for global

irradiance on a horizontal surface are presented in Figure 2-3. The figure is a product of the hourly values provided into the model.

Annual daily average irradiation in Ås is 2,536 kWh/m²/day. Annual maximum and minimum irradiance are 0,73kW/m² and 0kW/m² respectively. Sensitivity variables corresponding to ±40% of the annual average irradiation have been added into the model, and are presented in Table 2-9.

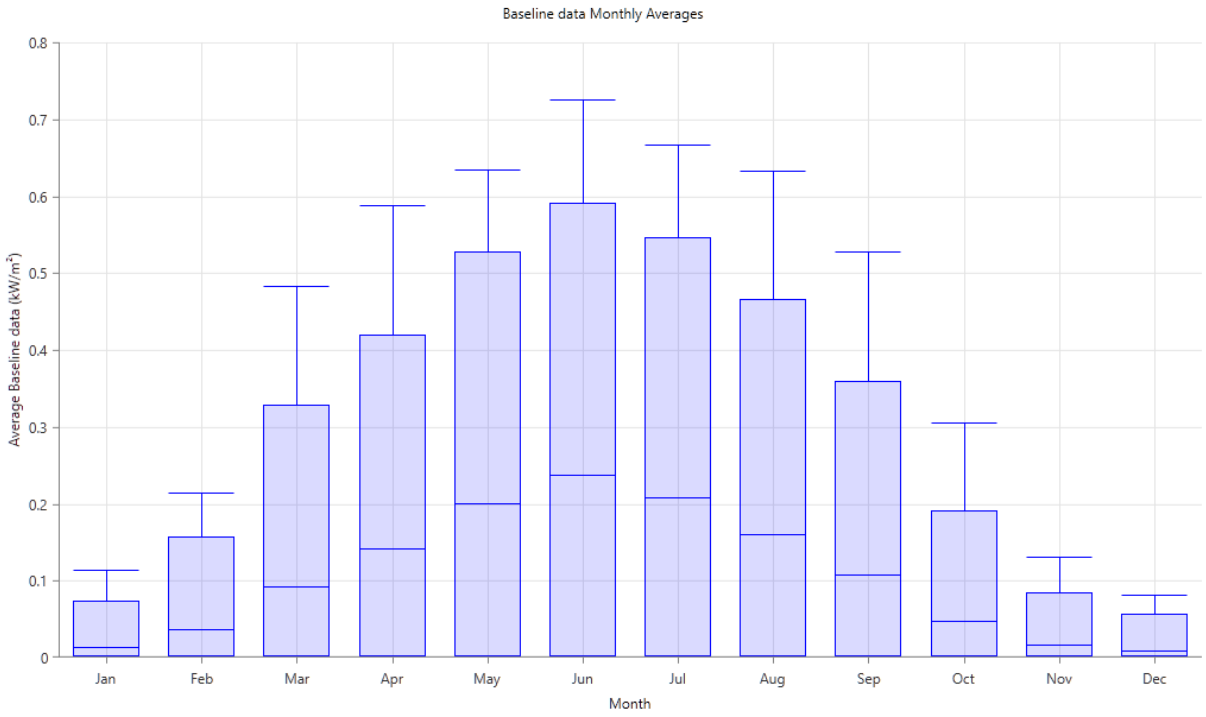

Figure 2-3: Annual monthly solar irradiance in Ås on a horizontal surface. The line at the top and bottom show the maximum and minimum values respectively. The line at the top and bottom of the blue box show the average daily maximum and minimum values. The line inside the box show the average monthly irradiance.

Inclination angle

When installing a PV array, one goal is to maximize the amount of radiation hitting the array. The inclination angle is relative to the ground surface, so installing the array horizontally equals to an inclination angle of 0°. In most cases, an inclination angle of 0° results in a lower amount of captured radiation than what is possible. The angle can either be fixed throughout the year, or

dynamically change by the help of solar tracking equipment optimizing the inclination according to the sun's position (Duffie & Beckman 2013 p.20).

Another type of radiation becomes influential when radiation on a tilted surface is considered; reflected radiation ($\bar{G}_r$). The amount of reflected radiation is determined by the surface type and cover. Albedo is a value used to describe the surface cover, and can vary throughout the year, especially in latitudes where snow precipitation is usual. HOMER use an annual average value, which is set to 36% as presented in Adaramola (2016). The stated value is relatively high, and is explained by snow cover in a large period of each year. Furthermore, the measurements are performed on a grass surface. Ideally, it should be possible to input reflectance values for smaller timesteps to account for annual variations.

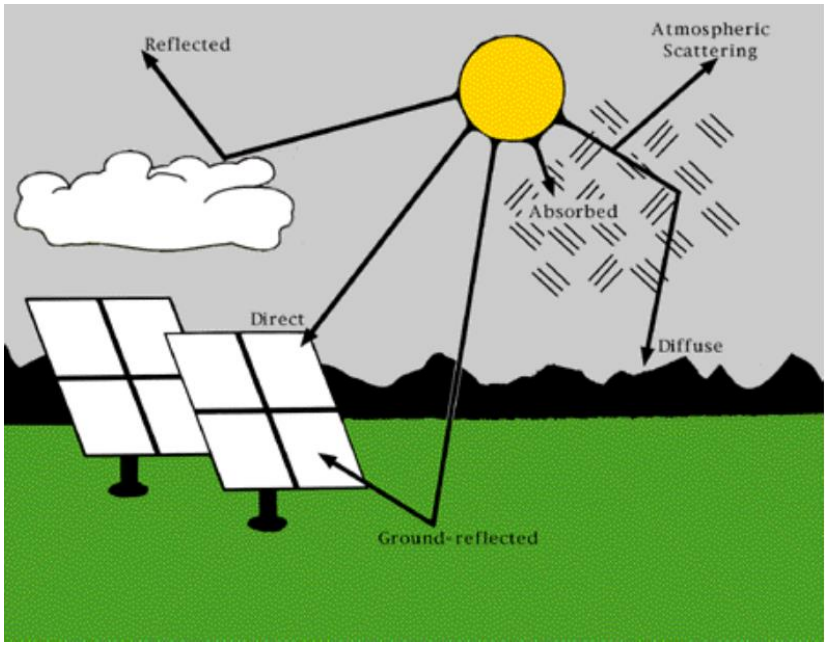

Figure 2-4: The relationship between direct, indirect (diffuse) and ground-reflected radiation. Reflected, absorbed and atmospheric scattered radiation does not hit the ground, and have not been mentioned in the thesis body (Homer Energy 2016 p.337).

Determining the inclination angle influences the power output throughout the year, and in return the total electricity generated. The amount of direct radiation is highest in the summer months, which imply that if the array is tilted to be perpendicular to the sun at solar noon in the summer months, the amount of

generated electricity would be maximized. This is not necessarily the case, because of other factors influencing power output, see chapter 2.5.1 for explanation on this.

The general rule when deciding the annually optimal inclination angle is to set the angle equal to the latitude of the installation site. Furthermore, by increasing or decreasing the inclination angle with 15°, the angle is adjusted to optimal winter or summer angle respectively (Messenger & Ventre 2005). A preliminary analysis of three inclination angles equal to 59,66°, 74,66° and 44,66° were performed in HOMER. An inclination angle equal to 44,66° returned the lowest LCOE, and was therefore chosen. Inclination angle was decided not to be a sensitivity variable in the main modelling, because inclusion increased the computational time considerably, and the sensitivity in relation to change in the optimal LCOE were considered less relevant compared to the other sensitivity variables included

Azimuth angle (γ) was set equal to 0°, meaning that the PV array is facing directly towards south. This is the angle that generally maximizes solar radiation incident on a tilted surface in the northern hemisphere (Duffie & Beckman 2013 p.24).

The monthly irradiance incident on the PV-array are presented in Figure 2-5.

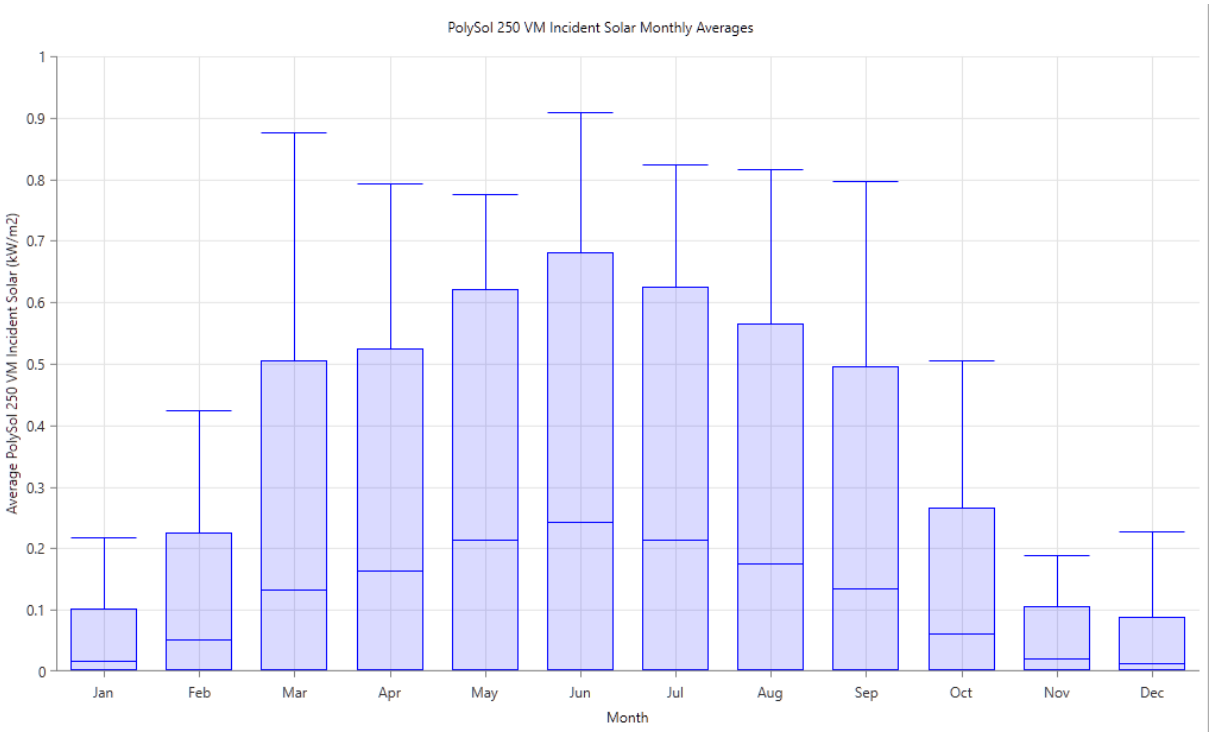

Figure 2-5: Annual monthly irradiance incident on the solar PV array. Top and bottom lines show the maximum and minimum values respectively. Top and bottom lines of the blue boxes show average of daily maximum and minimum values respectively. The line inside the box show the monthly average.

2.2.2 Temperature data

Ambient temperature is used to calculate the PV cell temperature. Since the temperature of the PV cells affects the power output of the PV-array, naturally the effect is important to include to achieve a more accurate result.

Average monthly temperature of the hourly data provided into the model can be seen in Figure 2-6. Scaled annual average temperature is 6,38°C. Annual maximum and minimum temperatures are 21°C and -9°C respectively.

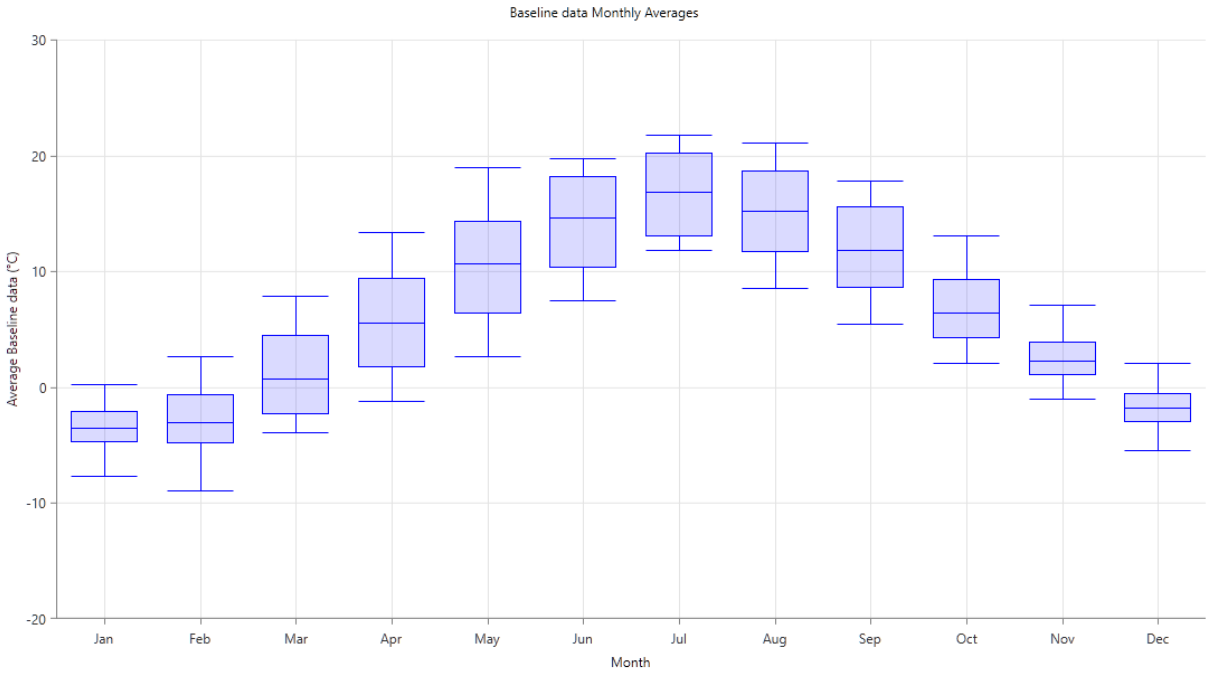

Figure 2-6: Maximum and minimum daily temperatures in each month are the top and bottom lines. The top and bottom of the blue box is the average of maximum and minimum values for each day in the respective months. The middle line is the daily average in each month.

2.2.3 Wind data

Wind speed is important for the power output of the wind turbine. To conduct the calculations dependent on the wind speed, three parameters needs to be provided.

Altitude above sea level is used to calculate the air density at the specific site. The altitude above sea level is set to 93,3 meters in the analysis, equal to the meteorological station's altitude (*Om FAGKLIM* 2017). Equation 3 is used to calculate the site-specific air density ratio.

$$\frac{p}{p_0} = \left(1 - \frac{Bz}{T_0}\right)^{\frac{g}{RB}} \left(\frac{T_0}{T_0 - Bz}\right) \quad (3)$$

Where:

$\frac{p}{p_0}$: air density ratio of site-specific air density (p) and standard air density (p_0). p_0 =1,225kg/m^3

B: lapse rate [0,00650 K/m].

z: altitude above sea level [m]. Set to 93,3 in this analysis.

T_0: temperature at standard conditions [288,16 K].

g: gravitational acceleration [9,81 m/s^2].

R: gas constant [287 J/kgK].

Wind speed measurements are performed at anemometer height. When the wind turbine is installed at a different height, known as hub height, the wind measurements must be adjusted. Mainly two different methods are used to adjust the wind speed to a specified height; power law profile and logarithmic profile. Logarithmic profile has been chosen in this analysis, and are calculated using Equation 4 (Homer Energy 2016 p.238; Koussa & Koussa 2015). Anemometer height is set to 10 meters (*Om FAGKLIM* 2017).

$$U_{hub,t} = U_{anem,t} * \frac{\ln\left(\frac{z_{hub}}{z_0}\right)}{\ln\left(\frac{z_{anem}}{z_0}\right)} \quad (4)$$

Where:

$U_{hub,t}$: wind speed at hub height at timestep t [m/s].

$U_{anem,t}$: wind speed at anemometer height at timestep t [m/s].

z_{hub}: hub height of wind turbine [m]. Set to 18 meters.

z_{anem}: height of anemometer [m]. Set to 10 meters.

z_0: surface roughness length [m]. Set to 1,5 meters.

Surface roughness length indicates the characteristic of the surface where the turbine is mounted. Since the analysis examines a hybrid electricity system for residential purposes, the surface type has been decided to be “Suburb”. Homer

Energy (2016 p.128) use values defined by Manwell et al. (2010 p.46) for different surface types, where the "Suburb" value equal to 1,5 meters. The resulting wind speed profile is presented in Figure 2-7.

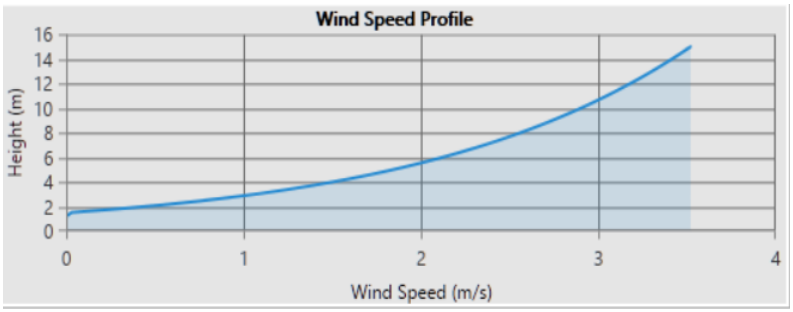

Figure 2-7: Wind speed profile with a roughness length of 1,5 meters. Derived from the wind speed data provided into the model, and based on the annual average wind speed.

The annual wind resource data is presented as monthly maximum, minimum, daily maximal and minimal average, and total monthly averages in Figure 2-8. Mark that the data is given in anemometer height. HOMER does not provide a visual presentation of the wind data at hub height, but the resulting power output from the wind turbine will reflect the effect from the wind speed profile.

Scaled annual average wind speed is 2,9 m/s. Annual maximum and minimum wind speed are 6,2 m/s and 1,0 m/s respectively. Two sensitivity variables corresponding to ±40% of the scaled annual average have been added to the analysis, and are presented in Table 2-9.

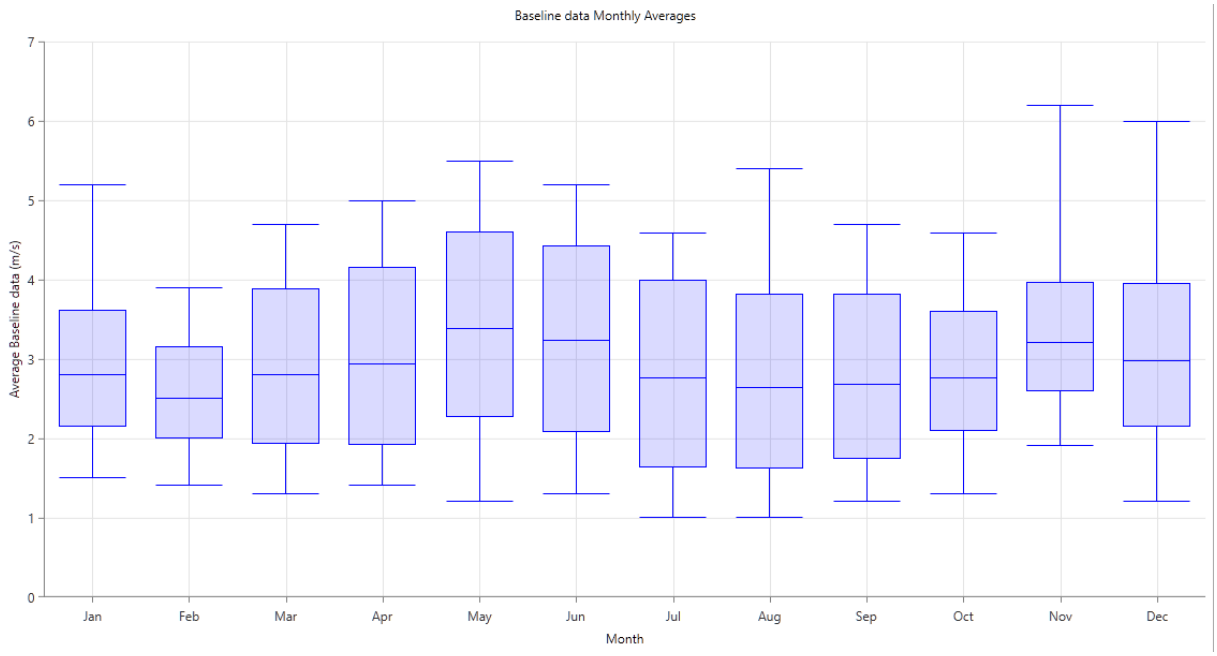

Figure 2-8: Wind resource at anemometer height provided into the model. The top and bottom lines in each month show the maximum and minimum wind speed respectively. The top and bottom lines in the blue boxes represent the average of daily maximum and minimum values respectively. The middle line represents the monthly average wind speed.

2.3 HOMER

The model used for conducting the analysis in this thesis is named Hybrid Optimization Model for Electric Renewables (HOMER). It is developed at the National Renewable Energy Laboratory (NREL) located in USA, and is created to easily design and compare different power generation technologies used for varying applications (Lambert et al. 2006 p.379).

The core elements of HOMER are visualized in Figure 2-9, where simulation of the system with different configurations are the first step. Second, multiple simulations are used to generate one optimization. Third, multiple optimizations are used to conduct one sensitivity analysis (Lambert et al. 2006 p.380).

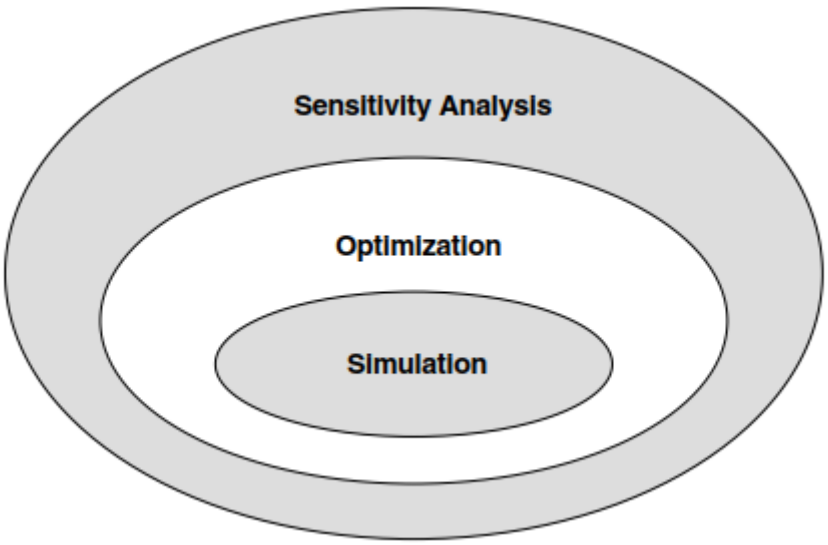

Figure 2-9: Illustration of the relationship between simulation, optimization and sensitivity analysis in HOMER.

The simulation process determines how a certain system configuration, hereunder included technologies and their specifications, will function over a specified period. This is done by using hourly data essential for the energy system to operate, like solar irradiance, wind speed and load demand. For each timestep in a year, the energy balance is calculated and summarized. The results make it possible to determine how much each technology is contributing in supplying the load, and how much excess or deficit energy that is generated. Excess energy can either be stored, sold to the grid, or dumped, depending on availability of storage technologies and if the system is grid-connected or autonomous. Energy deficit can be covered by generator, grid or stored energy. Exactly how the system operates is linked to what types of technologies that are evaluated, and the connected load types. Results from the simulation is used by HOMER to determine if the system is feasible in terms of meeting the constraints imposed by the modeler (Lambert et al. 2006 p.381-385).

Optimization uses the simulated results and ranks the different feasible systems based on the NPC. A lower NPC returns in a higher ranking of the system, meaning the objective function built into HOMER is to minimize NPC subject to determined constraints. With the objective in mind, HOMER returns different

variations of each system configuration, and optimized systems within each configuration is ranked and presented. Since the user do not know beforehand what component sizes that are optimal in each configuration, a selection of capacities and quantities, known as decision variables, are provided by the user. The basis are then set for HOMER to model and rank the systems (Lambert et al. 2006 p.385-388). A random example of optimization results from one sensitivity case can be seen in Figure 2-10.

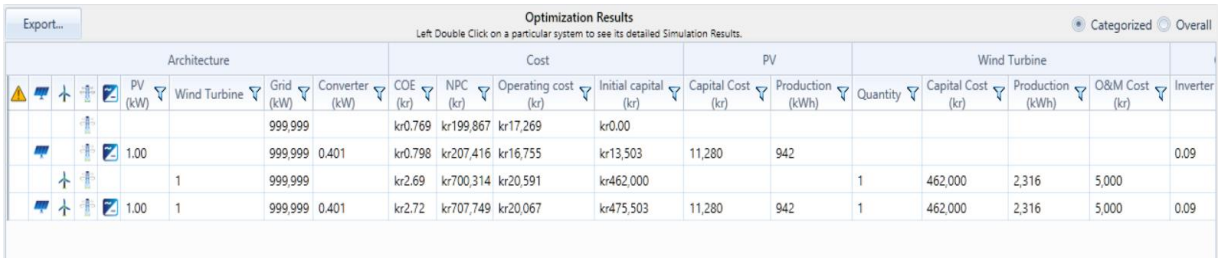
Export...

Optimization Results

Left Double Click on a particular system to see its detailed Simulation Results.

Categorized Overall

Architecture										Cost				PV		Wind Turbine				
				PV (kW)	Wind Turbine	Grid (kW)	Converter (kW)	COE (kr)	NPC (kr)	Operating cost (kr)	Initial capital (kr)	Capital Cost (kr)	Production (kWh)	Quantity	Capital Cost (kr)	Production (kWh)	O&M Cost (kr)	Inverter
						999,999		kr0.769	kr199,867	kr17,269	kr0.00							
				1.00		999,999	0.401	kr0.798	kr207,416	kr16,755	kr13,503	11,280	942					0.09
					1	999,999		kr2.69	kr700,314	kr20,591	kr462,000			1	462,000	2,316	5,000	
				1.00	1	999,999	0.401	kr2.72	kr707,749	kr20,067	kr475,503	11,280	942	1	462,000	2,316	5,000	0.09

Figure 2-10: Random example of optimization results from HOMER. This is the categorized results, meaning the optimal solutions based on NPC for each system configuration are shown. Each optimized result consists of multiple simulations, which can be seen when choosing "Overall" depicted in the figure.

Sensitivity analysis is conducted to examine changes in simulations and optimizations when sensitivity variables change. These can for example be capital cost on components, inflation, interest rate, lifetime of project, and so forth. Sensitivity variables are entered by the user, which can provide a sensitivity range that is assumed to be relevant for the different inputs. This makes it possible to account for uncertainty in the provided data, and formulate optimal solutions under different circumstances (Lambert et al. 2006 p.388-389). Figure 2-11 visualizes different sensitivity scenarios modelled in HOMER. The figure is only for illustration purposes.

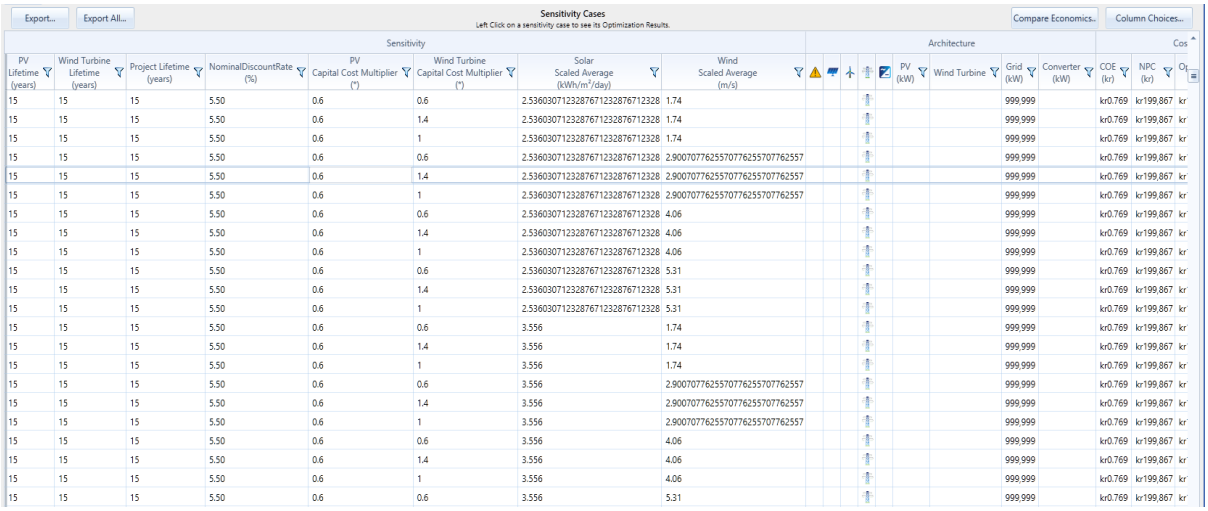

Figure 2-11: Example from HOMER showing a range of sensitivity cases performed. Each case has different combinations of sensitivity variables, which makes it possible to examine the impact of changes in both single and multiple variables simultaneously.

2.4 The hybrid energy system

This thesis examines the economic performance of a grid-connected electrical system, where utilization of solar PV and wind turbine are examined as possible technologies generating electricity. In order to clarify what is modelled, the system boundary is presented in Figure 2-12.

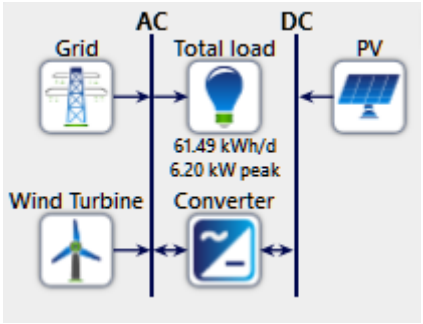

Figure 2-12: The modelled electrical system technologies, and its system boundary.

The figure illustrates what components that are modelled in this analysis. However, even though the load is within the system boundary, it results from a simulation of a model run exogenous of HOMER, and are therefore input data.

An elaboration on the load model and the resulting data are presented in chapter 2.1.

Outside of the system boundary is the meteorological resources and component prices of the various technologies. Meteorological resources and power prices are measured values, and not modelled within HOMER. Component prices are inputs presented in chapter 2.5.

2.5 Technologies

From the beginning of the work on this thesis, it has been a priority to use components that are available on the Norwegian market. In recent years, the interest for solar energy in Norway has increased, and so has the market for solar PV components (Ramsdal 2017). As a result, finding suitable components and associated prices for installing a solar PV system have been fairly easy, much because of the business register that the Norwegian Solar Energy Association has made available on their web page (*Bransjeregister* 2017).

In terms of finding a suitable wind turbine, the search has been more challenging. No register of available vendors of small scale wind turbines in Norway was found, and the general usage of this technology are not near the same popularity that solar PV have experienced. Initially, vertical wind turbines were explored to be used in the analysis, but after contact with the National Wind Energy Center (NVES) located at Smøla in Norway, I was recommended a horizontal turbine that they have installed for testing purposes at their premises (Bjørdal 2017). They had previously tested a vertical turbine that did not perform satisfactory, and because of their experience I chose to follow their advice.

2.5.1 Solar PV

The PV module used in the analysis is IBC PolySol 250 VM, a polycrystalline 250Wp module with a rated efficiency of 15,30%. The module has been chosen

from a selection of other modules offered by Solcellespesialisten because of the lowest cost per rated Wp. Module specifications used in the analysis, and search space for the component optimization, are presented in

Table 2-2, and further details are presented in attachment 1.

Table 2-2: Applied specifications for one IBC PolySol 250 VM module. All prices include VAT.

Parameter	Value	Unit
Power, peak capacity, Y_{PV}	0,25	kWp
Efficiency, $\eta_{mp,STC}$	15,30	%
Lifetime	25	years
Electrical bus	DC	(AC/DC)
Derating factor, f_{PV}	89,50	%
Temperature coefficient, α_p	-0,48	%/°C
Nominal operating cell temperature, $T_{c,NOCT}$	46,00	°C
Unit cost, incl. installation	5750	kr
Operation and mantainance cost	29	kr/year
Replacement cost	0	kr
Search space	0,0 1,0 3,0 5,0 7,0 9,0 10,0	kWp

Operating- and test conditions

There are two different environmental conditions that solar PV modules are rated under. Standard test conditions are specified to ensure that module specifications are comparable between producers, meaning that modules from one producer is tested under the same conditions as other producers. The standard test condition is defined in Table 2-3.

Table 2-3: Specified Standard Test Conditions (STC) for solar PV modules.

Specification	Value	Unit
Irradiance	1,0	kW/m²
Cell temperature	25	°C
Wind speed	0	m/s

The cell temperature ($T_{c,NOCT}$) is given under normal operating conditions. The normal operating condition is defined in Table 2-4.

Table 2-4: Specified normal operating conditions for solar PV modules.

Specification	Value	Unit
Irradiance	0,8	kW/m²
Ambient temperature	20	°C
Wind speed	1	m/s

Costs

Costs related solar PV modules consist mostly of an investment cost, which can be divided into component cost and installation cost. Since the solar modules do not consist of any moving parts, the operation and management costs are very low. It can be necessary to clear snow from the surface during periods when snow is present, and it may also be necessary to clean the panels in case of significant dusting, although this is not likely to be an issue because of frequent precipitation in the Ås area, and is not assumed to be a monetized operation cost for the system owner. The operation and maintenance cost is assumed to be 0,5% of the investment cost, corresponding to NOK29 (Multiconsult 2013 p.22).

A generalized investment cost distribution and its elements are presented in Figure 2-13. Mark that the inverter share included in the figure are linked to an average sizing ratio to the PV array. In this analysis, the sizing, and consequently cost, of the inverter is modelled separately from the PV module.

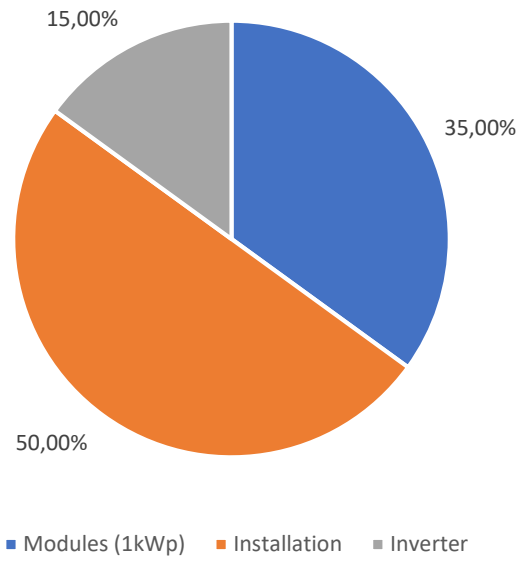

Figure 2-13: The distribution of costs and the main elements when investing in a 1kWp solar PV array in Norway (Multiconsult 2013).

The module cost is set to be 9452 $\frac{kr}{kWp}$ including VAT, collected from the webpage to Solcellespesialisten the 21. February 2017. The installation and equipment cost is assumed to be 50% of the total investment cost per kWp including inverter (Multiconsult 2013 p.18). The final investment cost for solar PV, without Enova funding and inverter cost, is presented in Equation 5:

$$C_{PV} = C_{module} + C_{install} = 23\,000 \frac{kr}{kWp} \tag{5}$$

Power output

The power output from the PV array is calculated for each time step with Equation 6 (Homer Energy 2016; Koussa & Koussa 2015):

$$E_{PV,T} = Y_{PV} f_{PV} \left(\frac{\bar{G}_T}{\bar{G}_{T,STC}} \right) \left[1 + \alpha_p \left(T_{c,T} - T_{c,STC} \right) \right] \tag{6}$$

Where:

$E_{PV,T}$: power output in current timestep [kW].

Y_{PV}: rated peak capacity of the array under standard test conditions [kW].

f_{PV}: derate factor of the array [%].

$\bar{G}_T$: irradiance incident on the PV array in current timestep [kW/m^2].

$\bar{G}_{T,STC}$: irradiance incident on the PV array under standard test conditions [1kW/m^2].

α_p: temperature coefficient of power [%/^{o}C].

$T_{c,T}$: cell temperature in current timestep [^{o}C].

$T_{c,STC}$: cell temperature under standard test conditions [25 ^{o}C].

Derating factor is included in the power output equation to account for electricity losses within the PV array and its wiring until the electricity enters the inverter (Homer Energy 2016 p.386). The derating factor can be separated into one temperature dependent factor and one temperature independent factor, and is formulated in equation 7 (Masters 2013 p.323-327):

$$f_d = f_{temp} * f_{no-temp} \tag{7}$$

Non-temperature related derating factors can be soiling, shading, electrical losses, or aging (Masters 2013 p.323). f_{temp} is calculated for each timestep in HOMER with equation (9). Since temperature degradation is modelled endogenously dependent on the hourly temperature, only $f_{no-temp}$ needs to be defined. To calculate $f_{no-temp}$, the value for f_d presented by Adaramola and Vågnes (2015 p.458), and f_{temp} presented by Adaramola and Quansah (2016 p.5) are used. The resulting derating factor is presented in Equation 8.

$$0{,}8303 = 0{,}928 * f_{no-temp} \rightarrow f_{no-temp} = \frac{0{,}8303}{0{,}928} * 100 \approx 89{,}5\% \tag{8}$$

There are three temperature related factors presented in

Table 2-2 that indicate the module performance at a given ambient temperature. A brief explanation of these are presented in the following sections.

Temperature coefficient of power, α_p [%/°C] indicates how much the PV array power output depends on the cell temperature (Homer Energy 2016 p.388).

Nominal operating cell temperature, $T_{c,NOCT}$ [°C] is the surface temperature that the PV array would have under normal operating conditions (Homer Energy 2016 p.387).

Efficiency at standard test conditions, $\eta_{mp,STC}$ [%] is the maximum power point efficiency under standard test conditions. The efficiency is also dependent on the cell temperature, but HOMER assumes that the maximum power point efficiency is equal to the efficiency at standard test conditions (Homer Energy 2016 p.232; Messenger & Ventre 2005 p.51-52).

Equation 9 show how the three aforementioned parameters are used for calculating the cell temperature at each time step (Duffie & Beckman 2013 p.758; Homer Energy 2016 p.232).

$$T_c = \frac{T_a + \left(T_{c,NOCT} - T_{a,NOCT}\right)\left(\frac{G_T}{G_{T,NOCT}}\right)[1 - \frac{\eta_{mp,STC}(1 - \alpha_p T_{c,STC})}{\tau\alpha}}{1 + \left(T_{c,NOCT} - T_{a,NOCT}\right)\left(\frac{G_T}{G_{T,NOCT}}\right)\left(\frac{\alpha_p \eta_{mp,STC}}{\tau\alpha}\right)} \qquad (9)$$

Where:

T_a: ambient temperature.

$T_{a,NOCT}$: ambient temperature at normal operating conditions [20°C].

G_T: solar radiation striking the PV array [kW/m^2].

$G_{T,NOCT}$: solar radiation striking the PV array under normal operating conditions [0,8 kW/m^2].

$T_{c,STC}$: cell temperature under standard test conditions [25°C].

τ *and* α: solar transmittance and solar absorptance respectively. The product of these two factors are assumed to be 0,9 by HOMER. The value are determined by Duffie and Beckman (2013 p.758).

2.5.2 Inverter

The inverter is chosen from a selection at Solcellespesialisten. It is produced by the German company IBC Solar AG, and has the model number SB 1300TL-10 (*SB 1300TL-10* 2017). Applied specifications of the inverter, and the search space for capacity optimization used in the model, are presented in Table 2-5. More detailed specifications are presented in attachment 2.

Table 2-5: Applied specifications related to inverter SB 1300TL-10 used in the analysis. All prices include VAT.

Parameter	Value	Unit
Power, peak capacity	1,4	kWp
Efficiency	94,30	%
Lifetime	15	years
Phases	1	#
Capital cost	5543	kr/kWp
Replacement cost (2017-price)	5543	kr/kWp
Search space	0,000 0,292 0,401 0,438 0,547 1,400 4,667 5,250	kWp

Sizing of the inverter is dependent on the potential savings or income that the inverter capacity enables, and so different capacities are considered. Sizing the inverter to meet the max output from the PV array is not necessarily beneficial, as the additional investment cost is not covered by the additional electricity generated.

Note that the search space specified in Table 2-5 mostly includes capacities that don't add up in integer quantities when they are divided by the peak capacity. This choice has been made because the focus in the thesis is directed towards capacities on solar PV and wind turbine, and capacities resulting in integer

quantities for the inverter would not give the minimal LCOE possible. The values used are results from running the HOMER optimizer, which is an proprietary algorithm that determines the optimal capacity for each simulation (Homer Energy 2016 p.143, 11). These values have been added into the search space method to reduce simulation time.

2.5.3 Wind turbine

The wind turbine used in the analysis is an Avance R9000 manufactured by Britwind. It is a horizontal-axis turbine rated at 5kWp.

Table 2-6: Applied specifications for the wind turbine used in the analysis. The values are given per turbine with tower, including VAT.

Specification	Value	Unit
Power, peak capacity	5	kWp
Lifetime	25	years
Hub height	18	m
Electrical bus	AC	(AC/DC)
Capital cost	330000	kr
Operation and maintenance	5000	kr/year
Replacement cost	0	kr
Search space	0 1 2	#

Power output

The real performance of a wind turbine is described by its power curve, which shows a relationship between the wind speed at hub height and the power output from the turbine. The power curve is presented in Figure 2-14, and is plotted from the certification document provided by Bjørdal (2017). Full certification summary is presented in attachment 3.

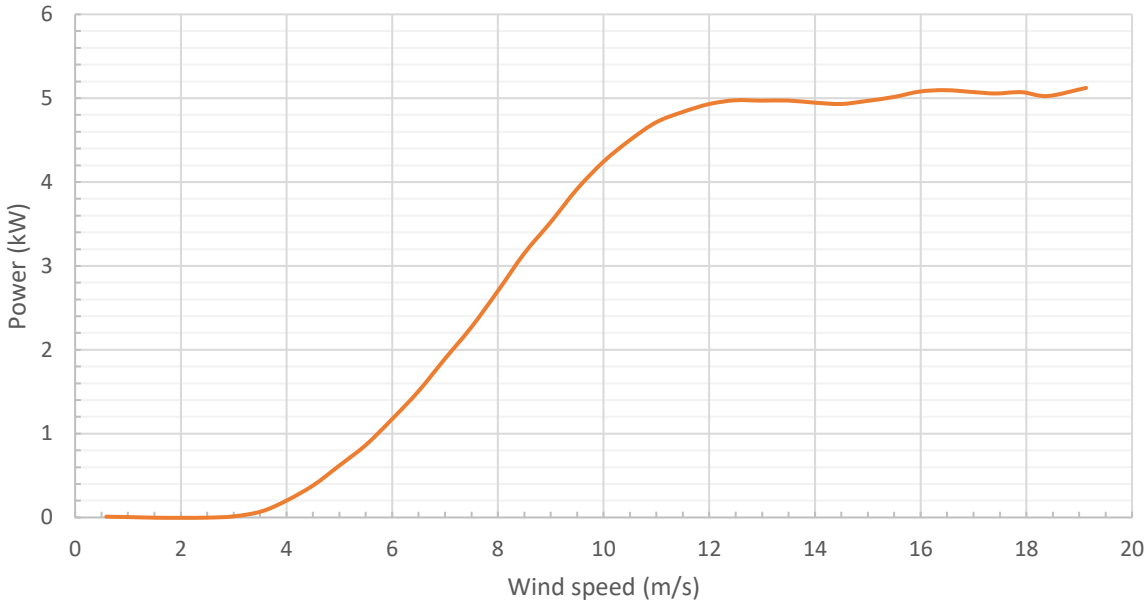

Figure 2-14: Certified power curve for the Evance R9000 manufactured by Britwind. Wind speed is given in hub height.

As for the specifications of the solar PV module, the specifications for the wind turbine is given at a specific set of conditions. The power curve is determined at a sea level air density of 1,225kg/m^3 and ambient temperature of 15 °C, meaning that the power output don't necessarily correspond to the power curve at an altitude different than sea level. Equation 10 is used for calculating the site-specific power output, where air mass ratio, presented in Equation 3, is included to account for change in air mass.

$$P_{WTG} = \left(\frac{p}{p_0}\right) * P_{WTG,STP} \tag{10}$$

Where:

P_{WTG}: wind turbine power output (kW)

$\frac{p}{p_0}$: air mass ratio

$P_{WTG,STP}$: power output at standard temperature and pressure (15°C and 1,225kg/m^3 respectively).

Costs

Costs affiliated with a wind turbine is dominated by investment in the turbine and tower, installation costs, and operation and management costs. When installing a wind turbine in the scale that is applied in this thesis, it is necessary to do some preparation work on the site in order to mount the tower and turbine.

The total investment cost is provided by Thomas Bjørdal at The Norwegian Wind Energy Center (NVES), and is given as 330 000NOK (Bjørdal 2017). The cost distribution is presented in Figure 2-15.

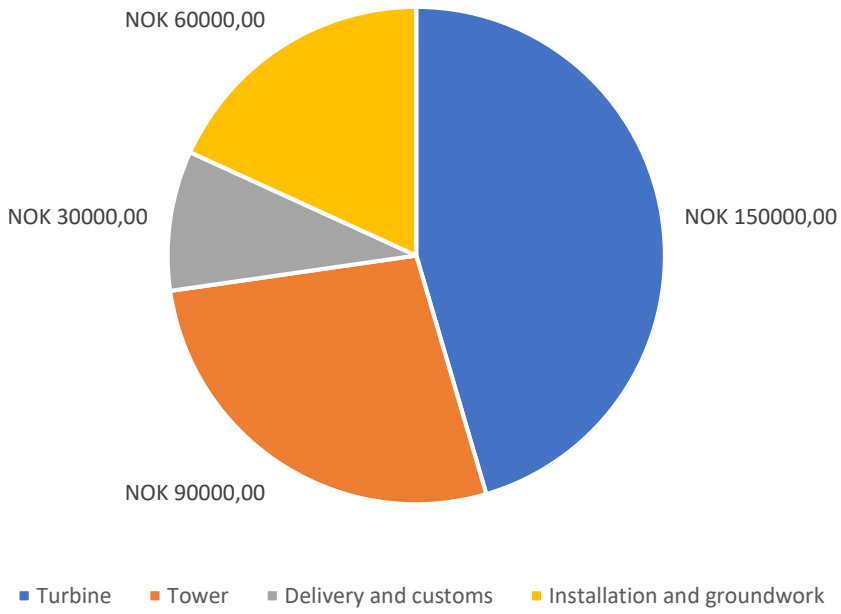

Figure 2-15: Prices for buying and installing one 5kWp Avance R9000 turbine in Norway. The prices are given in 2017 level, and includes VAT.

The operation and maintenance cost per year is given as NOK5000 (Bjørdal 2017). NVES is the Norwegian distributor of the wind turbine, so the prices are updated and realistic. Sensitivity variables corresponding to ±40% of the initial capital cost for the wind turbine have been added in the analysis. These are presented in Table 2-9.

2.5.4 Grid

There are five price areas in Norway, and the main market place for electrical power is run by Nord Pool. The areas exist because of bottle necks within the national electrical power grid, which can result in price differences between the areas. Ås are in price are NO1.

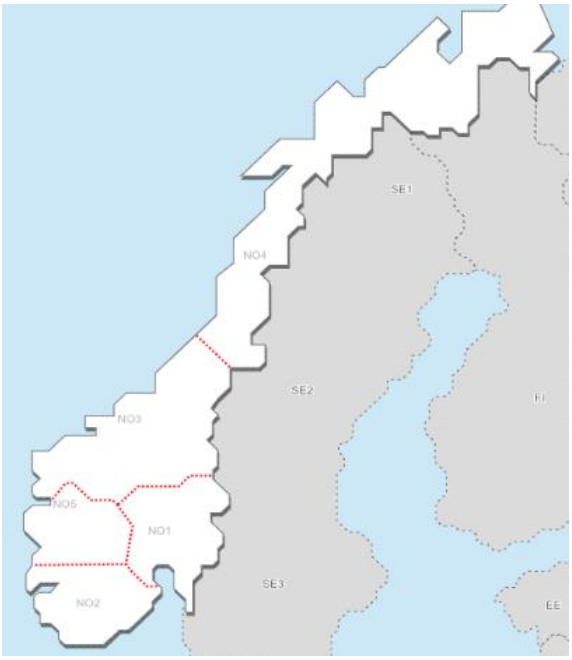

Figure 2-16: Illustration of the five price areas in Norway. The areas are marked with white (Prisområder 2016).

Grid power price

Elspot prices used in the analysis are collected from Nord Pool and includes hourly values from area NO1 from the years 2013 to 2016 (*Historical market* 2017). The data provided by Nord Pool are given as NOK/MWh, while HOMER demand the price values to be given in NOK/kWh, so the data have been changed correspondingly. Furthermore, the hourly values from each year have been summarized into an arithmetically mean for each timestep, and have resulted in 8760 average values. The hourly prices for each year are presented in Figure 2-17, and Figure 2-18 show the mean hourly elspot prices. Annual average elspot price is 0,235kr/kWh.

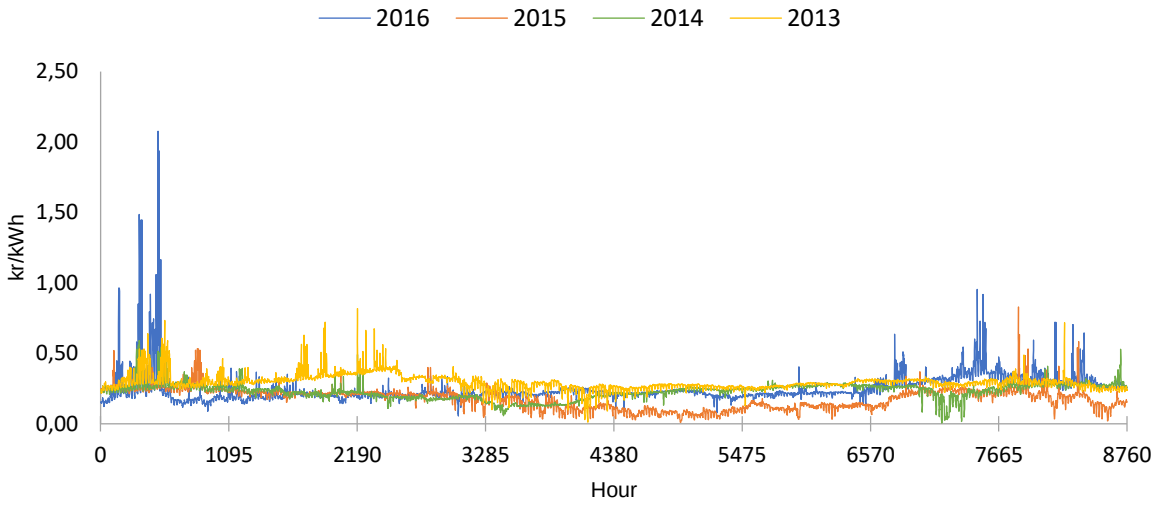

Figure 2-17: Hourly elspot prices in NO1 from year 2013 to 2016.

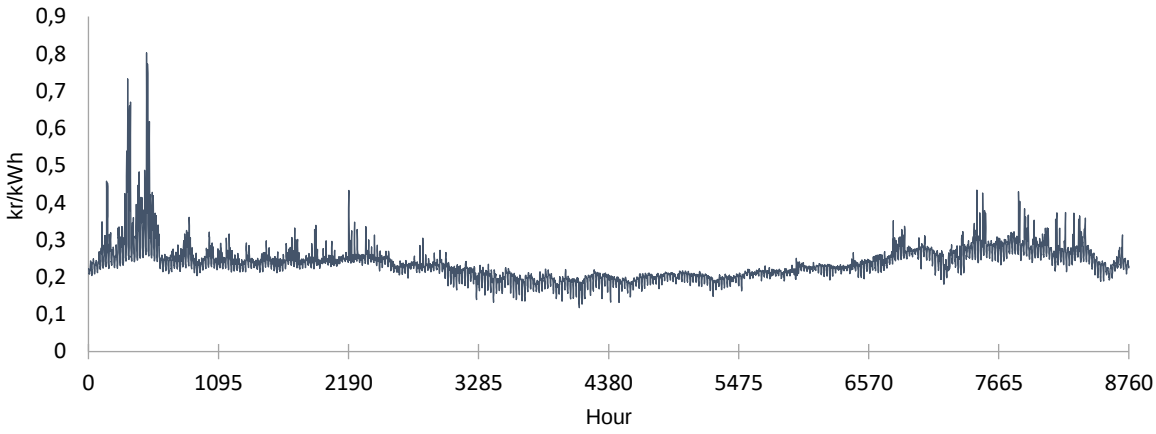

Figure 2-18: Mean hourly elspot prices used as a part of the grid power price in the analysis.

Hafslund Nett is the local grid operator in Ås municipality. The grid tariff is an operation and maintenance cost that the local grid operator charges the entities consuming electricity in their operation area, and is set at a yearly basis (*Historiske priser* 2016).

The grid tariff is a part of the grid power price used in the analysis, and is the arithmetically mean from year 2013 to 2016. As the tariff is set at a yearly frequency, the hourly values are constant throughout one year, and are therefore easily presented in Table 2-7.

Table 2-7: Grid tariff values used as a basis for the average grid tariff, which is included in the hourly grid power price. Including VAT and electricity tax.

Year	2013	2014	2015	2016	Average
Value [kr/kWh]	0,376	0,385	0,407	0,4505	0,405

Electricity tax is also a part of the grid power prices, and is set at an annual frequency (*Electric power* 2017). This tax is already included in the net tariff presented in Table 2-7, and will therefore not be specified.

Green certificates are a part of the grid power price for the consumers, and are included as a part of the grid power prices. The average certificate prices from year 2013 to 2015 are used and presented in Table 2-8. Green certificates can also be an income for an entity selling electricity to the grid. How this is handled in the analysis is presented in chapter 2.6.2.

Table 2-8: The annual average certificate prices for electricity consumers in Norway, including VAT. Used as a part of the hourly grid power prices.

Year	2013	2014	2015	Average
Value [kr/kWh]	0,012	0,021	0,025	0,019

To summarize, the grid power prices are input as hourly values into the analysis, and consists of prices on elspot, grid tariff, electricity tax, and green certificates. Elspot, grid tariff and green certificates includes VAT. Annual average grid power price is 0,719kr/kWh.

Finally, a yearly fixed fee for grid-connected households in Ås are included in the modelling. The fee is equal to NOK750 per year, and is the same for all the examined system configurations.

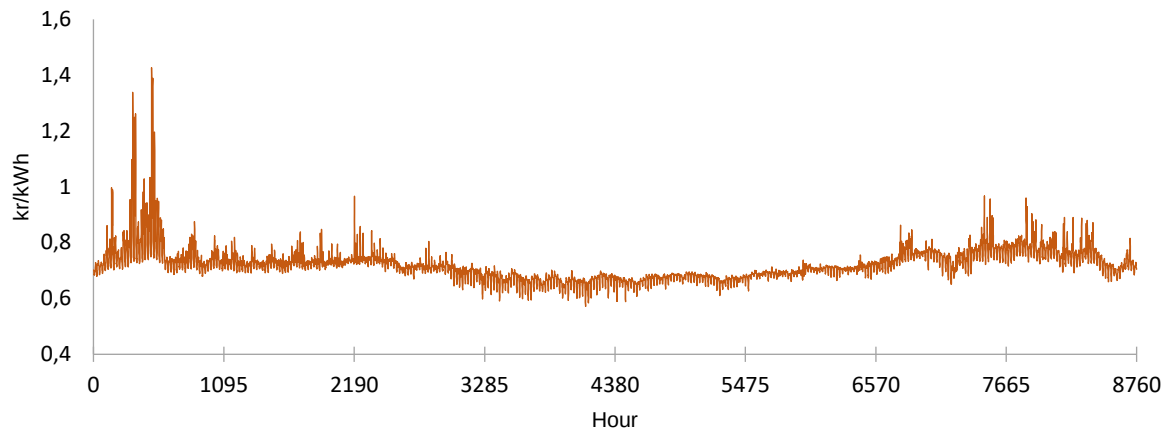

Figure 2-19: Hourly grid power prices that are used in the analysis, including VAT.

Grid sellback rate

The grid sellback rate is generally lower than the grid power price. To sell electricity, a deal must be made with an electricity provider in Norway. When the deal is signed the owner of the electricity generating equipment is defined as a prosumer ("plusskunde" in Norwegian) (Fladen 2016). By default, you receive the elspot price in the moment you sell electricity to the grid. The amount and time is registered, and is communicated to the power company involved in a contract with the owner of the distributed power system. In return, the seller receives the current market price on the sold electricity.

Currently it is possible to achieve a significantly higher grid sellback rate through one Norwegian power company named Otovo. They offer to buy for NOK1 per kWh, with an annual selling limit of 5000 kWh. If the limit is exceeded, you receive the respective market prices in the hours you sell additional excess electricity (*Våre betingelser* 2017). In this analysis, Otovo will be used as the entity buying excess electricity from the distributed system. However, two scenarios are examined. In scenario A, the grid sellback price is equal to 1kr/kWh, and constant through each year. In scenario B, the grid sellback rate are equal to the hourly elspot prices presented in Figure 2-18.

HOMER does currently not provide the ability to apply differential power prices at different sales quotas. As a result, in scenario A, only systems with a sold

quantity of electricity equal to or less than 5000kWh per year will be used in the analysis.

When calculating the arithmetic mean power price, the hourly values have not been adjusted for inflation between 2016 and the respective years. This may affect the final LCOE, but will not likely affect the rating of the optimal system configurations. Furthermore, an additional income from the local grid owner because of reduced loss in the distribution network have not been included as an income. This value is approximately 0,05kr/kWh (Bentzen 2017).

2.6 Economics

This analysis is using LCOE as the main metric for examining the potential electricity systems. The objective function is to minimize the LCOE, and the constraint is to meet the load demand in each timestep.

2.6.1 Investment subsidies

Currently an investment subsidy is received from Enova when installing equipment for local power production. Two different tariffs are applied, one that is given as a fraction of total cost, and one that is given per installed capacity in kilowatts. The investment subsidy is 35% of the total cost and up to 10000 NOK. As a result, if the total cost is above NOK28571, a flat subsidy of NOK10000 is provided. The subsidy per kilowatt peak is NOK1250, and runs up to 15 kilowatts peak capacity (*El-produksjon* 2016).

Currently, investment subsidies from Enova are applied to the whole distributed electricity system. Since HOMER only allows for input cost specifications on the individual technologies, net present cost and cost of energy including subsidies for the optimal systems will be calculated after the simulations have been conducted. However, the general expressions for total investment cost when receiving Enova subsidies are presented in equations 11, 12 and 13.

$$TC_{TS} = TC * (1 - 0{,}35) - \frac{1250}{kWp} \quad for\ TC \leq 28571 NOK\ and\ kWp \leq 15 \quad (11)$$

$$TC_{TS} = TC - 10000 - \frac{1250}{kWp} \quad for\ TC > 28571 NOK\ and\ kWp \leq 15 \quad (12)$$

$$TC_{TS} = TC - 28750 \quad for\ TC > 28571 NOK\ and\ kWp > 15 \quad (13)$$

2.6.2 Production subsidies

Green certificates are the subsidizing arrangement that Norway and Sweden jointly operates. The reason for its existence is to increase the electricity production from new renewable energy in the two countries by 28,4TWh within the end of year 2020. The support applies to new renewable capacities built from the 7. September 2009, including existing power plants increasing production capacity with an applicable renewable energy source. Hydro power plants built after 01. January 2004 are also applicable for receiving green certificates (Elsertifikatloven § 8).

When new capacity of renewable energy is set in operation, it receives a green certificate per MWh produced (Elsertifikatloven § 10). The certificate is then supplied into the market, and the entities selling electrical power must buy certificates corresponding to a certain quota that varies throughout every year until 2035 (Elsertifikatloven §§ 17 and 18).

Prosumers can apply for the right to receive green certificates from their excess electricity production. However, the cost for submitting the application is NOK15000 for systems with an installed effect below 100kWp (*Elsertifikatordningen er* 2016). Based on the average market price for the certificates from 2013 to 2017 of 165kr/MWh, the entry cost is assumed to be too high compared to the potential income from selling certificates (*Rapporter elsertifikater* 2017). As a result, green certificates will not be included as an income in the analysis.

2.6.3 Interest rate, inflation and project lifetime

Risk free nominal interest rate used in the analysis have been determined to be 5,5%. The interest rate represents the burden that investor experience as a result of binding the money in the project (Bøhren & Gjærum 2009 p.195). This depends on if the capital is retrieved through a loan, or if the capital alternatively can be invested in for example bank savings or stocks.

Inflation is set to 2,0% based on the historical development from 2006 to 2016 (*Inflation indicators* 2017). HOMER uses the real interest rate when calculating the NPC, since it assumes that all costs increase with the same rate equal to the inflation (Lambert et al. 2006 p.414). To calculate the real interest rate formula 14 is used (Bøhren & Gjærum 2009 p.174; Homer Energy 2016 p.362).

$$i = \frac{i' - f}{(1 + f)} \tag{14}$$

Where

i = real interest rate

i' = nominal interest rate.

f = expected inflation.

Project lifetime is decided to be 25 years because of the assumed lifetime of both wind turbine and solar PV module are set to 25 years. This results in neither the wind turbine or the solar PV module being replaced during the project lifetime, and their scrap values will be equal to NOK0. The inverter will be replaced after a period of 15 years, and will have a scrap value at the end of the project period.

Because the financial variables are uncertain, sensitivity variables on interest rate and project lifetime have been added into the model. These are presented in Table 2-9.

2.6.4 Levelized cost of energy and net present cost

HOMER calculates several economical metrics when running the simulations, but total net present cost is the metric that it uses to compare and rate different system configurations. Total net present cost (NPC) is defined as the present value of all costs minus the present value of all revenue during the project's lifetime (Homer Energy 2016 p.409). It is important to note that NPC is depicted as a positive number in the results, although NPC practically is negative in relation to the term net present value (NPV) (Lambert et al. 2006 p.414). NPC is calculated by using equation 15 (Bøhren & Gjærum 2009 p.193):

$$C_{NPC,co} = \sum_{t=0}^{T} \frac{X_t}{(1+r)^t} \tag{15}$$

Where:

T: the project lifetime

t: year of calculation

r: interest rate, either real (i) or nominal (i').

X_t: net cost in year t, either in nominal or real prices for the component.

$$C_{NPC,sys} = \sum_{co=1}^{n} C_{NPC,co} \tag{16}$$

Equation 15 is used on each individual component in the electric energy system, where each component's capital, replacement, maintenance and fuel cost, in addition to revenues like salvage value and sold electricity are summarized. When each component's NPC are determined, denoted by $C_{NPC,co}$ where "co" is the component type, they are summarized into the total net present cost of the system with Equation 16. The annualized cost for the system is calculated using

the capital recovery factor (CRF), depending on the lifetime and the interest rate of the project. CRF is presented in Equation 17:

$$CRF(i,N) = \frac{i(1+i)^N}{(1+i)^N - 1} \tag{17}$$

Annualized cost for the system is calculated using Equation 18:

$$C_{ann,tot} = C_{NPC,sys} * CRF(i,N) \tag{18}$$

Finally, the levelized cost of energy is calculated using Equation 19 (Lambert et al. 2006 p.415):

$$LCOE = \frac{C_{ann,tot}}{E_{prim} + E_{def} + E_{grid,sales}} \tag{19}$$

Where:

E_{prim}: the annual primary load that the system must meet.

E_{def}: annual deferrable load, which is load that does not need to be met at specific times throughout one year. Is not assigned in this analysis.

$E_{grid,sales}$: annual electricity sold to the grid.

2.7 Sensitivity variables

There are a number of sensitivity variables applied to examine the impact different variables have on the results. This is important to achieve a better understanding of the impact that possible under- or overestimation have on the results.

Note that sensitivity values for lifetimes on project, PV-modules and wind turbine are linked together in the analysis. This means that simulation of change

in these variables have been conducted simultaneously, so for example a reduction in project lifetime also impose reduction in PV and wind turbine lifetime. The link between these three variables have primarily been created in order to reduce simulation time, and these three variables are the most logical to experience a simultaneous change.

All the sensitivity variables considered are presented in Table 2-9.

Table 2-9: Sensitivity variables used in the analysis.

Change	-40%	0%	40%
Project lifetime	15	25	35
PV lifetime	15	25	35
Wind turbine lifetime	15	25	35
Nominal discount rate	3,3	5,5	7,7
PV capital cost multiplier	0,6	1,0	1,4
Wind turbine capital cost multiplier	0,6	1,0	1,4
Solar scaled average	1,524	2,536	3,556
Wind scaled average	1,74	2,90	4,06

3 Results

In chapter 3.1 I will present the optimal systems corresponding to the measured meteorological data presented in chapter 2.2, and the component costs that have been presented in chapter 2.5. Chapter 3.2 presents optimized LCOEs including investment subsidies, and chapter 3.3 presents sensitivity analyzes of systems B5 consisting of grid, 5kW wind turbine and 10kW solar PV array, and B4 consisting of grid, 5kW wind turbine and 1kW solar PV array.

3.1 Optimized system configurations

The following results are based on the assumptions presented in Table 3-1.

Table 3-1: Assumptions that are basis for the results presented in subsection 3.1.

PV lifetime	25	Years
Wind turbine lifetime	25	Years
Project lifetime	25	Years
Nominal discount rate	5,5	%
Inflation	2,0	%
PV capital cost multiplier	1,0	(*)
Wind turbine capital cost multiplier	1,0	(*)
Solar scaled average per year	2,536	kWh/m²/day
Wind scaled average per year	2,900	m/s

The HOMER-analysis was conducted for two different scenarios, depicted scenario A and B. The reason was that it was not possible for HOMER to conduct sensitivity analyzes on grid power prices and sellback rates given in hourly timesteps. As a result, the effect of different selling prices could not be presented without conducting simulations and optimizations for two different selling price scenarios. Scenario A assumed a fixed selling price of NOK1 per hour. Scenario B assumed selling prices as the elspot price values for their respective timesteps presented in Figure 2-18.

3.1.1 Scenario A – Sell price as 1 kroner

HOMER returned feasible simulated systems with four different configurations. Additionally, HOMER presented optimized options for each configuration. System A1 consisted of Grid only, system A2 consisted of Grid and PV, system A3 consisted of Grid and Wind turbine, and system A4 and A5 consisted of Grid, PV and Wind turbine. The optimized results are presented in Table 3-2.

Table 3-2: Optimized results based on a selling price of 1NOK/kWh. All electricity generation values are given per year.

S/No.	S_{config}	$E_{purchased}$	E_{sold}	E_{PV}	E_{Wind}	P_{PV}	P_{wind}	P_{inv}	NPC (kr)	LCOE (kr/kWh)
A1	Grid	22445	-	-	-	-	-	-	286749	0,77
A2	Grid + PV	21617	-	942	-	1	-	0,40	305249	0,82
A3	Grid + Wind	20138	8	-	2316	-	5	-	671909	1,80
A4	Grid + PV + Wind	19341	43	942	2316	1	5	0,40	690245	1,85
A5	Grid + PV + Wind	15886	4548	9423	2316	10	5	5,25	837630	1,87

System A5 generated a notable amount of electricity sold to the grid, and are examined further in chapter 4.2 by using Figure 3-1. Annual development on key variables like load, grid sales, grid power price, renewable power output from the wind turbine and PV-array and the grid sellback rate will be used as a basis for the discussion.

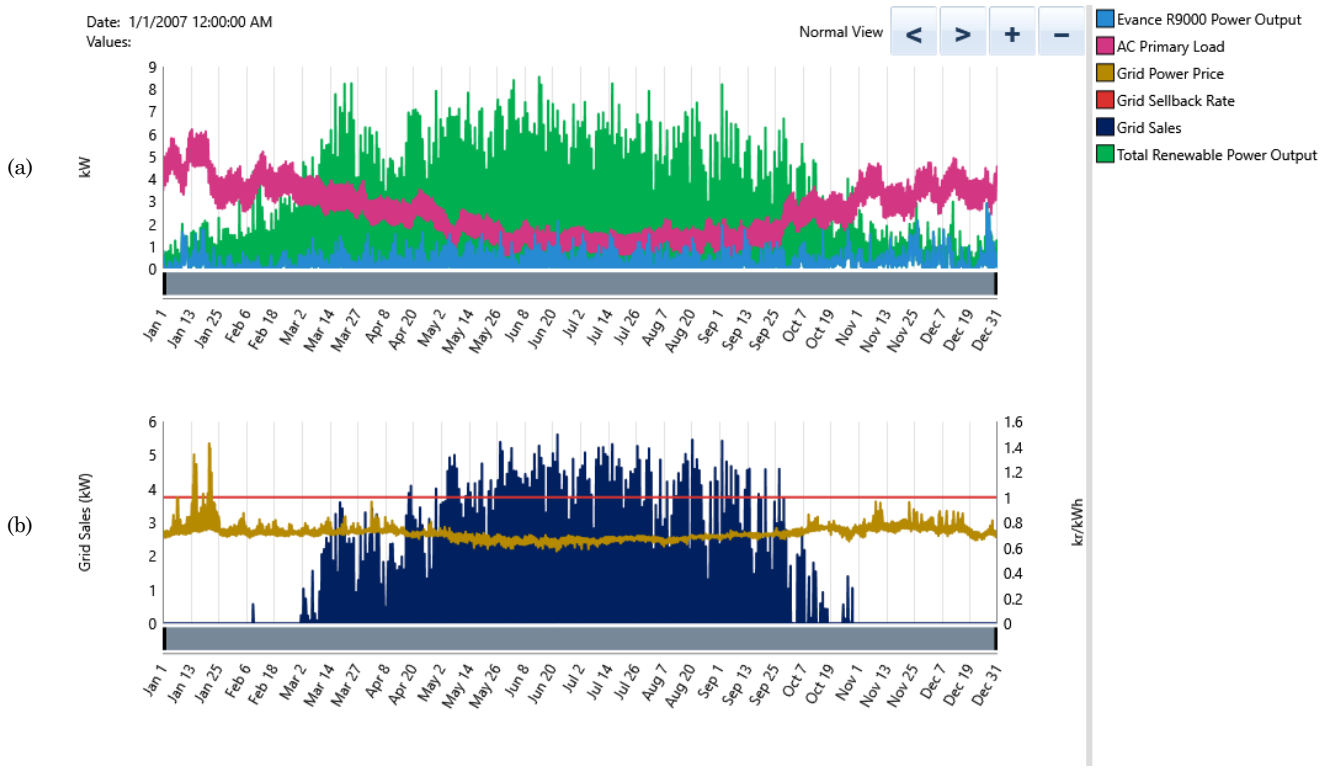

Figure 3-1: Load profile, total renewable power output and wind turbine output in (a). Grid sales, grid power price and grid sellback rate in (b). Power output in the figure applies specifically to system A5, and the sellback rate applies only to the scenario A-systems.

3.1.2 Scenario B – Sell price as hourly spot price

Optimized results for Scenario B are presented in Table 3-3. The same system configurations as in scenario A are present, although with slightly different values for the net present costs in systems 1 to 4. LCOE in scenario A and B for systems 1 to 4 are equal.

Table 3-3: Optimized results based on selling prices equal to the hourly elspot prices presented in Figure 2-18. All values on electricity generation are given per year.

S/No.	S_{config}	$E_{purchased}$	E_{sold}	E_{PV}	E_{Wind}	P_{PV}	P_{wind}	P_{inv}	NPC (kr)	LCOE (kr/kWh)
B1	Grid	22445	-	-	-	-	-	-	286749	0,77
B2	Grid +PV	21617	-	942	-	1	-	0,40	305249	0,82
B3	Grid + Wind	20187	8	-	2316	-	5	-	672639	1,80
B4	Grid + Wind + PV	19391	39	942	2316	1	5	0,40	691391	1,85
B5	Grid + Wind + PV	15933	4546	9423	2316	10	5	5,25	897108	2,00

The annual development in key variables for system B5 are presented in Figure 3-2, and will be used for comparison with system A5 presented in Figure 3-1.

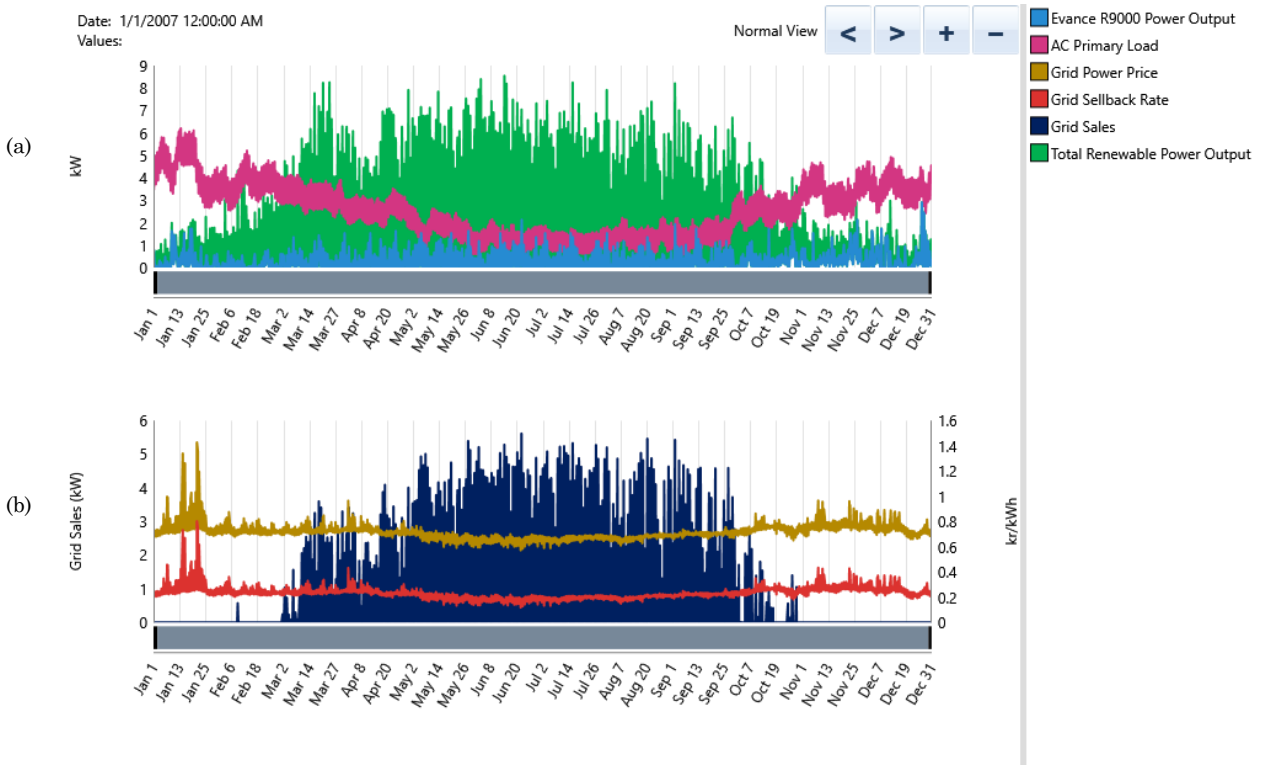

Figure 3-2: Load profile, total renewable power output and wind turbine output in (a). Grid sales, grid power prices and grid sellback rates in (b). Power output applies specifically to system B5, and the sellback rates applies to all scenario B-systems.

3.2 Results including Enova subsidies

When the optimal systems were determined, it was possible to calculate the NPC and LCOE when including subsidies from Enova for each result. Formulas and values used in the calculation can be found in chapter 2.6.3. The final costs for each optimized system are presented in Table 3-4.

Table 3-4: NPC for the optimized systems when including Enova support corresponding to the systems initial capital cost and installed effect. Used as basis for calculating LCOE including subsidies.

S/No.	Initial capital	P_{PV}	P_{wind}	Subsidy	$NPC_{S,tot}$	$C_{ann,tot}$	E_{served}
A1 and B1	-	-	-	-	286749	17266	22445
A2	25223	1	-	10079	295171	17773	22445
A3	330000	-	5	16250	655659	39480	22453
A4	355223	1	5	17500	672745	40509	22484
A5	589100	10	5	28750	808880	48706	26993
B2	25223	1	-	10079	295171	17773	22445
B3	330000	-	5	16250	656389	39486	22453
B4	355223	1	5	17500	673891	40540	22484
B5	589100	10	5	28750	868965	52287	26993

Changes in LCOE values before and after including subsidies are presented in Figure 3-3.

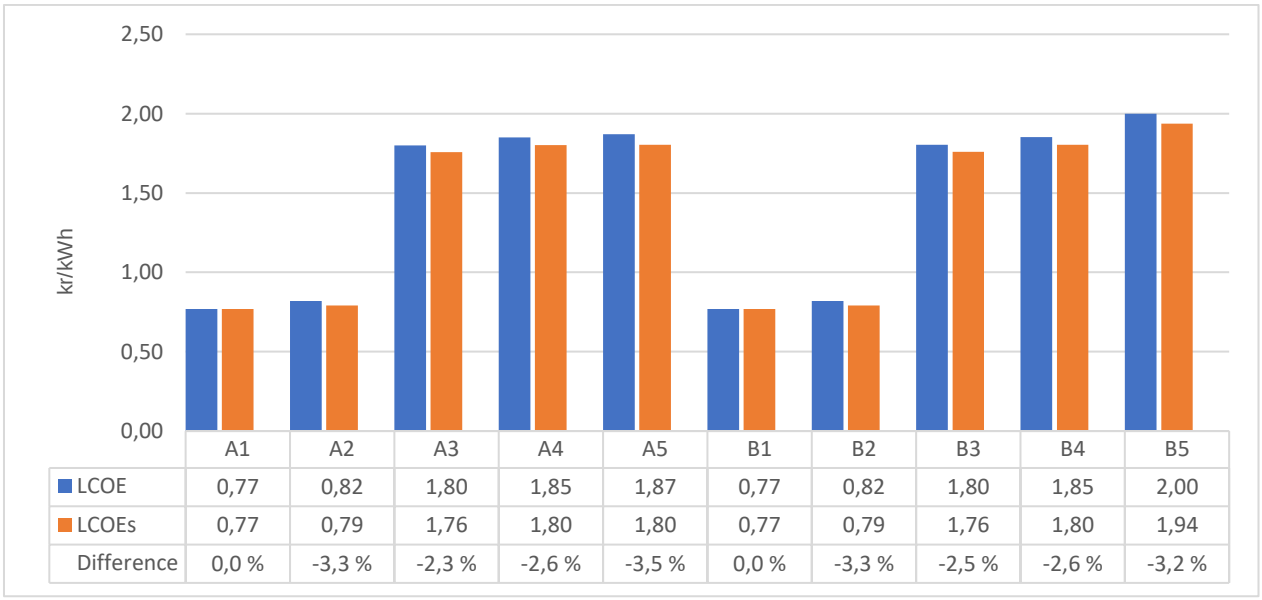

	A1	A2	A3	A4	A5	B1	B2	B3	B4	B5
LCOE	0,77	0,82	1,80	1,85	1,87	0,77	0,82	1,80	1,85	2,00
LCOEs	0,77	0,79	1,76	1,80	1,80	0,77	0,79	1,76	1,80	1,94
Difference	0,0 %	-3,3 %	-2,3 %	-2,6 %	-3,5 %	0,0 %	-3,3 %	-2,5 %	-2,6 %	-3,2 %

Figure 3-3: LCOE values with and without ENOVA subsidies corresponding to the installed capacity and investment cost for the respective systems. The LCOE from both scenarios are shown.

3.3 Sensitivity analyzes

Many different systems were simulated in this analysis. Sensitivity analysis is built into HOMER, but are mostly focused on examining the effect on the optimal solutions. Obviously, there were potentially many sensitivity charts can could be presented. As the focus was to examine the benefits from utilizing multiple

energy sources, sensitivity charts on system B5 and B4 are presented. These were used to examine which variables affected the LCOE the most, and if system B5 could achieve a lower LCOE than B4 based on the same changes.

As previously mentioned, the grid sellback rate used in scenario A were not applicable when sold electricity exceeded 5000kWh. When conducting the sensitivity analysis on the optimal hybrid system in scenario A, this constraint would return inaccurate results when considering variables that increased electricity sold to the grid above 5000kWh. In order to overcome this problem, the hybrid systems B5 and B4 were evaluated, since the constraint was not applicable to scenario B.

Note that there are two lines representing changes in both wind and solar resource separately, and one line representing changes in both wind and solar resource simultaneously. This have also been done for change in capital cost for solar PV and wind turbine.

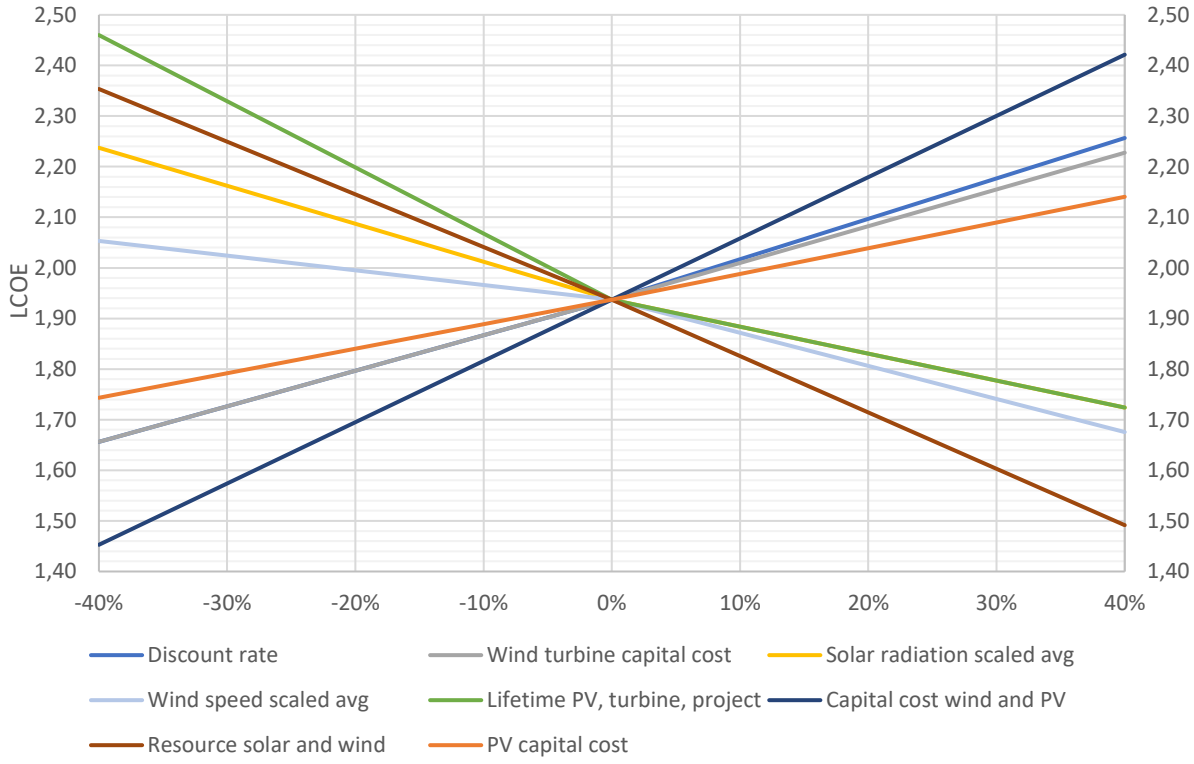

Figure 3-4: Sensitivity chart for system B5 – Grid + PV (10kW) + Wind turbine (5kW). Note that eight different variables are described, but only seven lines are present on each side of the graph. "Solar radiation scaled avg" are overlapped by "lifetime PV, turbine, project" in the range 0% to 40%. "Discount rate" are overlapped by "wind turbine capital cost" in the range 0% to -40%.

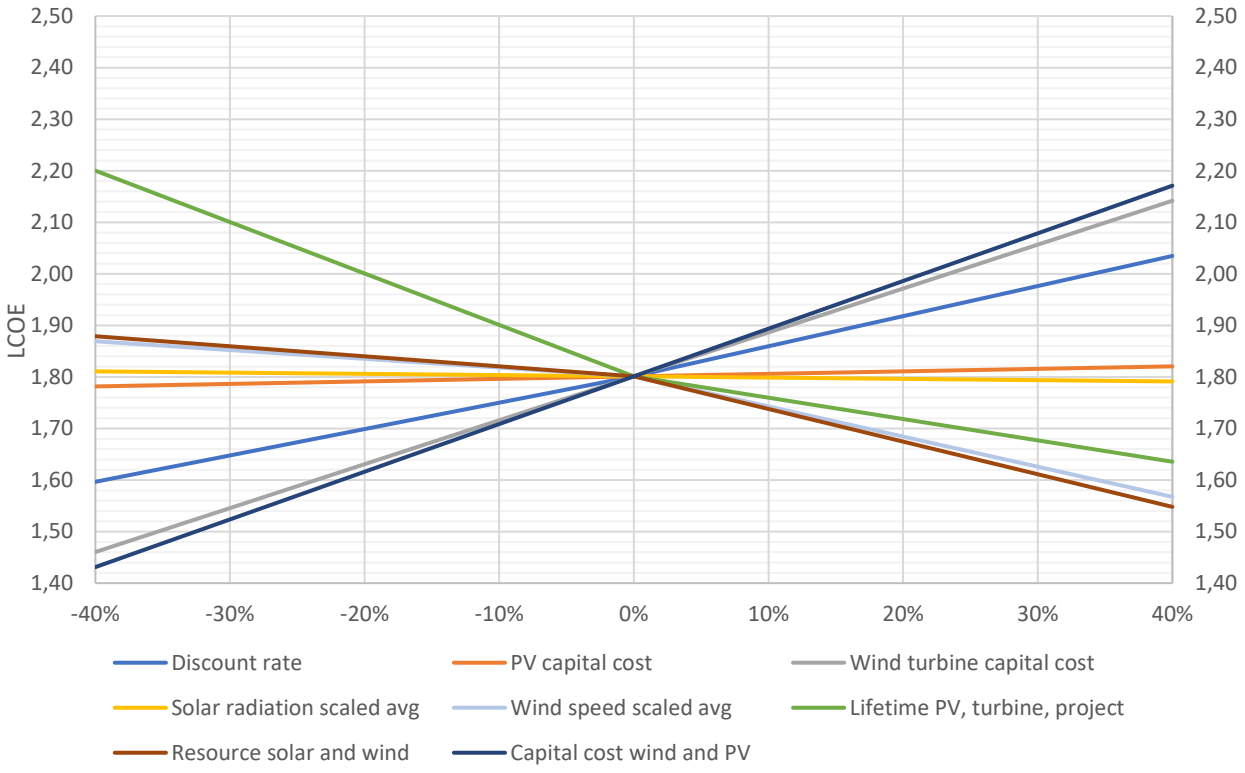

Figure 3-5: Sensitivity chart for system B4 – Grid + PV (1kW) + Wind turbine (5kW).

4 Discussion

4.1 Optimal system configurations

Findings presented in Table 3-2 and Table 3-3 clearly states that the grid-only configuration was the least cost alternative in both scenarios, with a LCOE of 0,77kr and NPC of 286749kr. Although these results depend on site-specific assumptions, two similar cases are presented in Dalton et al. (2009) and Akinyele et al. (2014).

Dalton et al. (2009) performed simulations on different grid-connected electric configurations including wind turbine, solar PV and batteries meeting the load of a large hotel, and found that with power prices from 2004, grid-only configuration resulted in the lowest NPC. However, it was stated that under expected increase in grid power price, a hybrid configuration of wind generator rated at 1,8MW and grid would be most economically viable. It should be noted that wind turbine cost per kW was lower than the PV cost per kW. Furthermore, the annual average wind speed was 5,85m/s while the wind turbine had a cut-in wind speed of 3m/s and a higher power output than the turbine used in this thesis. Finally, the resources data were hourly values only based on the year 2004, and consequently may not represent the real expected resource conditions at the site in a medium to long term.

Akinyele et al. (2014) performed an optimization analysis on identical system configurations examined in this thesis, but with other input values. They compared optimal system configurations at two scenarios with different constant grid sellback rates, and found that grid-only returned the lowest LCOE in the scenario with the lowest grid sellback rate. In the other scenario, a hybrid configuration of grid and wind turbine returned the lowest LCOE. The wind and solar resources presented in the case area were better than the location examined in this thesis, and the difference between investment cost per kW for the solar PV array and wind turbine were significantly smaller than presented in this thesis. Although it is not stated in the article, it is assumed that the wind turbine used

had a higher capacity factor than the PV array, contrary to the findings presented in this present analysis.

The results showed that installing technologies utilizing local energy sources to generate electricity was not profitable for a single household when considering monetized values at the applied available resources in Ås. System configurations including renewable technologies did show a reduction in electricity bought from the grid, but the reduced grid electricity expense did not cover the additional investment cost that the renewable power technologies entailed. This conclusion coincided with Koussa and Koussa (2015), who observed that a grid power price of 3$/kWh was necessary in order achieving an optimal system configuration including local power generating technologies.

Because the grid power price was simulated at an hourly resolution, it was not included in the sensitivity analysis. This was because of a constraint in HOMER that only made it possible to conduct sensitivity analysis on power prices given as annual average values. This was however shown to be an important sensitivity variable in Dalton et al. (2009) and Türkay and Telli (2011) in terms of change in optimal system configuration from grid-only to combined grid and HRES, and would be interesting to investigate in further research.

Although the optimal system did not include renewable energy technologies, the increase in installed capacity of solar PV in Norway have significantly increased in recent years (Ramsdal 2017). This could indicate that there are other benefits not measured in money that could result in an optimal system configuration including locally installed wind turbine, solar PV array, or a combination of the two. These benefits could for example be increased satisfaction and a perception of decreasing personal GHG-emissions (Jung et al. 2016).

4.2 Energy balance throughout one year

To examine the energy balance, the 15kW hybrid configuration consisting of 10kW solar PV array and 5kW wind turbine are used as an example, as it clearly

showes when the different technologies generated electricity during one year. The explanation use Figure 3-1 to illustrate, showing system A5.

From the grid sales curve shown in Figure 3-1(b), nearly no electricity was sold from the system between 01. November to approximately 01. March. However, there was power output in the period, mainly from the wind turbine. This resulted in a reduced need for purchasing electricity from the grid, in a period where the grid power price was at its peak. This effect was dampened by a high load demand in the same period.

Moving further into the year, the power output started to exceed the load demand in the start of March, and continued to the end of October. Because of the constant sellback rate in scenario A, the income per kWh was not dependent on time of day or year. It can be observed from Figure 3-1(b) that the grid sellback rate was significantly higher than the grid power price, which included taxes and the grid tariff.

When system B5 was considered in Figure 3-2, the grid sellback rate in Figure 3-2(b) are given in hourly changing values. This systems income from grid sales depended on the price development throughout the days and year. It is evident that the majority of sold electricity coincided with a period characterized by a generally low grid sellback rate, which affected the income significantly compared to system B5. This effect is discussed in more detail in Chapter 4.3.

Figure 3-2(a) shows the total renewable power output and the wind turbine output, and it can be easily observed that the solar PV contributed to the main power generation in total, especially in the spring and summer months. This is not surprising, as the PV array had the highest rated capacity, and that the irradiation increased throughout spring and summer, before it was reduced in the fall. Additionally, the annual capacity factor for the PV array was calculated to be 10,73%, while the wind turbine had an annual capacity factor of 5,29%. The capacity factor is defined in Equation 20 (Homer Energy 2016 p.161):

$$\frac{P_{avg}(kW)}{P_{rated}(kW)} * 100 = Cp(\%) \tag{20}$$

This is a result of generally low wind speeds throughout the year, an assertion reinforced by the 7833 hours of operation per year, compared to the PV array which was 4362 hours per year. The wind turbine capacity factor is highly dependent on the wind speed, a fact reflected in the non-linear power curve, so a stable but low wind speed results in a low capacity factor. Consequently, it can be stated that the resource basis for electricity generation from solar PV was more favorable than from the wind turbine.

Table 4-1: Generated electricity from PV-array and wind turbine during one year from system number 5. The electricity balance is equal in both scenarios.

Month	**PV el (kWh)**	**WT el (kWh)**	**Cp_{PV}**	**Cp_{Wind}**
Jan	121	168	1,62%	4,51%
Feb	330	60	4,91%	1,79%
Mar	921	160	12,38%	4,30%
Apr	1074	207	14,91%	5,76%
May	1413	358	18,99%	9,63%
Jun	1519	296	21,10%	8,22%
Jul	1379	166	18,54%	4,45%
Aug	1134	130	15,25%	3,49%
Sep	867	134	12,04%	3,72%
Oct	422	152	5,67%	4,09%
Nov	135	245	1,88%	6,81%
Dec	86	242	1,16%	6,50%

The hybrid system configuration allows for utilizing different energy sources at the same location, and the availability of the two sources determines the performance of the two technologies throughout the year. It can be seen in Table 4-1 how the different technologies contributed to the total renewable output, both on the amount of electricity generated and the capacity factor for the respective technologies. Variability in the capacity factor of the PV-array was stronger compared to the wind turbine. Although the wind turbine had a more stable capacity factor, its annual capacity factor was lower, and the wind turbine's maximum capacity factor value coincided with the maximum capacity factor value of the PV-array in May and June. In conclusion, the power output from the

wind turbine in periods with low output from the PV-array was not sufficient to cover the additional expenses that accompanied the wind turbine.

4.3 Significance of grid sellback rate

Grid sellback rate proves to be essential when a system generates a notable amount of electricity that exceeds load demand. However, it did not affect the optimal system rating when sorted after rising LCOE, as presented in Table 3-2 and Table 3-3.

Akinyele et al. (2014) performed a comparison with two different sellback rates, and found that the analysis including the highest sellback rate resulted in a change of the optimal system configuration, changing from grid-only to grid and wind turbine. However, the annual average grid power price used were 0,232USD/kWh (2kr/kWh), much higher than the average grid power price of 0,719kr/kWh in this analysis. Furthermore, unlike in the present study thesis, the grid power price in Akinyele et al. (2014) was not modelled in hourly timesteps. Finally, the amount of electricity sold from the grid and wind turbine configuration was 7311 kWh/yr, significantly higher than in this thesis.

Dalton et al. (2009) displayed the development in NPC for a system consisting of grid and wind turbine, when changes occured in both grid sellback rate and grid power price. At grid sellback rates equal or higher than the grid power price, the NPC development for the grid and wind turbine configuration was less steep than grid-only. This indicates that investing in local power generation may be economically viable as long as the grid sellback rate is higher than the grid power price. However, as the results in this thesis show, this also depends on the locally available energy resources (for examples, location's average wind speed and global radiation as well as their distribution), and the investment and labour cost, as well as existing level of infrastructure development.

When considering the lowest LCOE possible in each optimized system configuration between scenario A and B, the values presented in Figure 3-3 are

equal in both scenarios for system 1 to 4. Keeping in mind that the only factor separating the two scenarios are the grid sellback rate, this can be explained by the amount of electricity sold to the grid. System 1 is grid-only, and was naturally not affected by the sellback rate. System 2 and 3 sold 8kWh and 39kWh respectively to the grid annually, and compared to the annual capital and operations costs, the income from the sales are negligible.

When $LCOE_s$ for systems 5A and 5B are considered and compared, the significance of grid sellback rate becomes evident. System A5 and B5 generated the same amount of electricity, but the difference in $LCOE_s$ between the two systems are presented in Equation 21.

$$|LCOE_s(A5) - LCOE_s(B5)| = |1{,}80kr - 1{,}94kr| = 0{,}14kr \quad (21)$$

This gap in LCOE value would increase until the systems met the threshold of selling 5000kWh to the grid, although the rate of increase is decided by the difference in spot price in the hour useable electricity generation exceeds the load. From that point, the two systems would receive the same price per kWh sold, since they are identical in configuration and share the same available resources.

The grid sellback rate has a high significance for the profitability of distributed electricity systems, but the degree of significance depends on the amount of electricity sold to the grid. This is similar to observation made by Akinyele et al. (2014).

4.4 Effect of Enova subsidies

Investment subsidies did not change the rating of the different system configurations in relation to LCOE, and the hybrid configurations did not prove to be more economically profitable compared to the single-source configurations.

When subsidies were included, it can be seen in Figure 3-3 that the difference in LCOE within each system gave the most significant decrease in systems A5 and B5. This was a natural consequence from having the highest installed peak capacity, and therefore achieving the maximum subsidy. Note that when subsidies were included, system A5 achieved the same LCOE as system A4, even though the initial capital cost for system A5 was substantially higher. There are two reasons that can explain the levelled $LCOE_s$'s. System A5 received 11250kr more in subsidies than A4 because of the higher installed capacity. Furthermore, system A5 had a significantly higher amount of sold electricity to a grid sellback rate of 1kr/kWh.

When considering the parameters used for deciding the amount of subsidies granted by Enova, there were a discrepancy between generated electricity and received subsidies. Whether a system consisted of 15kW installed wind capacity, solar PV capacity, or a combination of the two, the amount of subsidies would still be NOK28750. As the results show, the capacity factor for the two technologies differed in favor of solar PV, meaning that 15kW would generate more electricity than 15kW wind power under the environmental conditions presented in this analysis. The discussion in chapter 4.2 shows that a hybrid configuration, of wind turbine and solar PV-array, made it possible to generate power over a longer period during one year. If this effect is desired by Enova, it should be considered to differentiate between distributed systems utilizing single- and multiple energy sources. Furthermore, when considering the substantial investment cost for the wind turbine used in this analysis, the need for subsidies were much higher than for the PV array in order to become economically viable. However, this fact can change if the wind turbine is deployed at locations with more favorable wind conditions than what are presented in this analysis.

4.5 Sensitivities for system B5 and B4

The optimal system configurations did not change when a sensitivity analysis was conducted on the variables listed in Table 2-9, so grid-only maintained its position as the optimal solution. However, examining the sensitivities of systems B5 and B4 can uncover a possible change in optimized hybrid system rating. Systems B5 and B4 are both hybrid systems with different power ratings, and consequently different investment costs and potential power generation capacities. Under the standard system inputs in Table 3-1, system B5 was less economically viable than B4.

Generally, it was evident that the combined sensitivities of resource basis and capital costs were the two variables that had the greatest impact on the LCOE for the two systems. However, lifetime of PV, turbine and project were most significant when the variables were decreasing.

Adaramola (2014) observed a significant decrease in LCOE when considering an increase in the global solar radiation in a hybrid grid and PV configuration, indicating the importance of the available energy resources. Furthermore, Saheb-Koussa et al. (2011) observed a significant decrease in NPC as a result of increased average wind speed in a hybrid grid, wind turbine and PV configuration. It was emphasized that the grade of sensitivity depends on the rated power output of the respective technologies in the system.

Reduction in capital cost for both wind turbine and solar PV modules were found to have a significant effect on the LCOE according to study reported by Türkay and Telli (2011), where 50% reduction for both technologies returned a 15% reduction in LCOE. It should be mentioned that investment cost in PV was more significant than wind turbine in Türkay and Telli (2011).

Comparing the sensitivities for system B5 and B4, the different variables showed the relatively same impact on the respective systems, meaning that the order of the majority of sensitivity lines were equal. However, the significance of discount rate was greater than wind turbine capital cost in B5. Explanation for this are linked to the rated capacity, and consequently higher amount of sold electricity to

the grid. Higher discount rate results in money used in the future becoming less worth, and in relation to system B5 the value of income from grid sales were decreased. Additionally, because of higher investment cost for system B5 in year zero, increasing interest rate returned a higher annual capital cost. Change in annual capital cost was greater for system B5 than B4, and consequently the impact of change in LCOE was more significant than for system B4.

All changes in the sensitivity variables imposed a more significant effect on the LCOE in system B5 than B4. Investment costs and potential production capacity were both higher in system B5, therefore system B5 was more disposed to uncertainty in the input data. However, the higher sensitivity for system B5 had the potential of achieving a lower LCOE compared to system B4 if the combined resource basis increased approximately 30%. Change in annual average wind speed were common for both systems, because both systems had the same wind power potential. The difference is presented in the higher installed effect of solar PV. When the sensitivity lines for annual average wind speed and combined average wind speed and solar radiation were compared, they were nearly the same in system B4. However, in system B5 the gap between them were much larger. Difference in these gaps illustrates that system B5 had the potential of utilizing more of the available solar resources than system B4, and that a 30% increase for both resources resulted in system B5 becoming more economically viable than B4.

4.6 Simplifications and limitations

HOMER did have the ability to conduct multi-year analysis on the data, meaning that it could for example include annual degradation of solar cell efficiency, or specific annual increase in power price. When activating this option, the simulation time increased to 19 hours. When simulation time was above 1 hour, the model would at several times crash, and as a result multi-year analysis was omitted.

The average elspot price is expected to increase to around 50-60€/MWh in 2030, which correspond to approximately a doubling of the average elspot price used in this analysis. This can have implications for the resulting LCOE values, and can affect the rating of the optimal system configurations. However, prices during the summer months are expected to be reduced because of increased capacity unregulated electricity technologies during the period. Lower prices at times when the main amount of electricity is sold from distributed electricity systems may reduce the profitability for unregulated distributed power generation. As a result, the significance of a high sellback rate, as used in scenario A, may increase in order to achieve an acceptable LCOE (Statnett 2017). Furthermore, the grid tariff is expected to increase around 30-50% towards 2023 compared to tariffs in 2014. The degree of tariff increase in the respective grid areas depends on the area-specific investment costs. In this regard, the main part of investments will be done in the eastern part of Norway, indicating that net tariff will increase considerably in the Ås-area. However, the degree of increase also depends on the population growth in each individual grid area (Sørgard et al. 2014).

Although the cost for PV-module are collected from a market vendor in 2017, the installation and equipment costs are calculated based on figures from Multiconsult (2013). Installation and equipment costs are based on the share of total costs as described in the report, and this share may have changed since the report was published. Because of the relatively substantial increase in installed solar PV capacity in Norway the last three years, there have likely been a learning effect related to installation (Kost et al. 2013; Ramsdal 2017). However, the sensitivity analyzes do likely cover some of the uncertainty in investment costs.

The load data used in this thesis are modelled values. An exact picture of the load in different households in Ås can only be obtained by using real metered data. When distributed electricity generation are considered for a specific household, the load data for the household in question should be used as basis for the calculations in order to achieve an optimized system design.

Resource basis for the renewable technologies presented in this thesis are not representative for Norway as a whole. The wind resources are much lower compared to a number of other places in Norway, and consequently the results can give an impression that small scale wind turbines are not suitable for distributed power generation, although this may not be the case when other locations are examined.

5 Conclusion and recommendations

This thesis has explored the economic feasibility of renewable electricity generation from grid-connected solar PV-modules and wind turbines. On the basis of the findings, some conclusions and recommendations are presented.

Grid-only was the system configuration with the lowest levelized cost of energy, showing that a consumer that is only interested in monetized costs should not invest in local power generation, provided that the assumptions presented in this thesis holds. However, the LCOE of grid-only and grid+PV configurations in both scenarios were 0,77kr/kWh and 0,82kr/kWh respectively, showing that the difference in costs were not considerably large. Furthermore, local power generation may involve benefits not included in the calculations. This can justify installation of a PV-array.

A renewable hybrid configuration of PV and wind turbine did increase the number of hours that power was generated annually. However, the additional costs affiliated with installing the wind turbine were too high compared to the additional benefit received. Benefits consisted of income from selling additional electricity to the grid, and cost savings from a reduced need of buying electricity from the grid.

By using two scenarios with different grid sellback rates, it was shown that grid sellback rate was highly important for the LCOE of distributed systems that sell a large amount of electricity to the grid. It was shown that the PV-array mainly generated power when the grid power price was low. As a result, receiving a price on excess electricity above the average power price in the summer months would reduce the LCOE compared to scenarios with grid sellback rates equal to the hourly spot prices.

Investment subsidies did not facilitate for grid-connected hybrid systems, as long as investment cost per kW was higher for one technology than the other technology. The amount of subsidies did not depend on the performance of the individual technologies, meaning that the support scheme did not necessarily support projects that generated the most renewable electricity.

The same sensitivity variables for the hybrid system configurations were equally important in both the 6kW configuration and 15kW configurations. However, the effect of change in each variable were more significant for the LCOE in the 15kW hybrid configuration (system B5), compared to the 6kW hybrid configuration (system B4). The combined sensitivities for capital cost and resource basis were most important when increase in variables were considered. At decrease in variables, combined lifetimes for project, PV-array and wind turbine, and combined capital cost were most important. If the combined resource basis increased with 30% or more, the LCOE for the 15kW hybrid configuration (system B5) became lower than the 6kW hybrid configuration (system B4).

5.1 Future research

When the sensitivity analyzes were conducted, probabilities of changes in the different sensitivity variables were not considered. Including probability in the analysis can show which sensitivity variables that should be considered in more detail.

The load provided into this analysis have only considered a single household. Considering installation of distributed generation that is shared by multiple households could be of interest, as the substantial investment cost could be more feasible when divided between multiple households. Furthermore, combining multiple loads can result in more of the generated electricity being consumed at the site instead of being sold to the grid, increasing both system efficiency and potentially reduce electricity costs.

Examine the complementation between solar radiation and wind speed at various locations in Norway. Compare power output from hybrid systems and single source systems, and how the output is distributed during the year. Better wind resources may provide more electricity output at times when the grid power prices are high, and consequently favor the wind turbine more than what is presented in this thesis.

Consider the benefit of distributed power generation for power grid utilities and the society. Local power generation may reduce the need for upgrading existing power grid, loss in transmission lines, and building new structures affecting environmental values.

6 References

Aanensen, T. & Olaisen, W. (2016). *Elektrisitetspriser*. Available at: https://www.ssb.no/statistikkbanken/selecttable/hovedtabellHjem.asp?KortNavnWeb=elkraftpris&CMSSubjectArea=energi-og-industri&checked=true (accessed: 07.05.2017).

Adaramola, M. S. (2014). Viability of grid-connected solar PV energy system in Jos, Nigeria. *International Journal of Electrical Power & Energy Systems*, 61: 64-69.

Adaramola, M. S., Agelin-Chaab, M. & Paul, S. S. (2014). Analysis of hybrid energy systems for application in southern Ghana. *Energy Conversion and Management*, 88: 284-295.

Adaramola, M. S. & Vågnes, E. E. T. (2015). Preliminary assessment of a small-scale rooftop PV-grid tied in Norwegian climatic conditions. *Energy Conversion and Management*, 90: 458-465.

Adaramola, M. S. (2016). Distribution and temporal variability of the solar resource at a site in south-east Norway. *Frontiers in Energy*.

Adaramola, M. S. & Quansah, D. A. (2016, September 07-09). *Comparative performance analysis of two small-scale grid-connected solar PV systems under tropical and temperate weather conditions*. International Conference of Mechanical Engineering, Ibadan, Nigeria.

Akinyele, D. O., Rayudu, R. K., Nair, N. K. C., Chakrabarti, B. & Ieee. (2014). Decentralized Energy Generation for End-Use Applications: Economic, Social and Environmental Benefits Assessment. *2014 Ieee Innovative Smart Grid Technologies - Asia (Isgt Asia)*: 84-89.

Bentzen, A. (2017). *Re: Godtgjørelse for redusert nettap* (e-mail to Vegard Bøe 03.05.2017).

Bernal-Agustín, J. L. & Dufo-López, R. (2009). Simulation and optimization of stand-alone hybrid renewable energy systems. *Renewable and Sustainable Energy Reviews*, 13 (8): 2111-2118.

Bjørdal, T. (2017). *Små vindturbiner til bruk i boligområder* (email to Vegard Bøe 23.02.2017).

Bøhren, Ø. & Gjærum, P. I. (2009). *Prosjektanalyse: Investering og finansiering*. Bergen: Fagbokforlaget. 530 pp.

Bransjeregister. (2017). Available at: http://finnsolenergi.no/ (accessed: 28.02.2017).

Dalton, G. J., Lockington, D. A. & Baldock, T. E. (2009). Feasibility analysis of renewable energy supply options for a grid-connected large hotel. *Renewable Energy*, 34 (4): 955-964.

Deshmukh, M. K. & Deshmukh, S. S. (2008). Modeling of hybrid renewable energy systems. *Renewable and Sustainable Energy Reviews*, 12 (1): 235-249.

Duffie, J. A. & Beckman, W. A. (2013). *Solar Engineering of Thermal Processes*. 4th ed. New Jersey: John Wiley & Sons, Inc.

El-produksjon. (2016). Available at: https://www.enova.no/privat/alle-energitiltak/solenergi/el-produksjon-/ (accessed: 09.03.2017).

Electric power: tax rates. (2017). Available at: http://www.skatteetaten.no/en/business-and-organisation/duties1/electric-power/ (accessed: 25.04.2017).

Elsertifikatloven. (2012). *Lov om elsertifikater*. Available at: https://lovdata.no/dokument/NL/lov/2011-06-24-39 (accessed: 06.03.2017).

Elsertifikatordningen er gebyrfinansiert. (2016). Available at: https://www.nve.no/energiforsyning-og-konsesjon/elsertifikater/kraftprodusenter/gebyr/ (accessed: 28.04.2017).
Fladen, B. A. (2016). *Endringer i kontrollforskriften vedrørende plusskundeordningen: oppsummering av høringsuttalelser og endelig forskriftstekst*. Oslo: NVE. 20 s. pp.
Hansen, H., Eggum, E., Ånestad, A. & Aabakken, C. (2017). *Avbrotsstatistikk 2016*. Avbrotsstatistikk, vol. 2017:43. Oslo: Norges vassdrags- og energidirektorat. Available at: http://publikasjoner.nve.no/rapport/2017/rapport2017_43.pdf (accessed: 11.05.2017).
Historical Market Data. (2017). Available at: http://www.nordpoolspot.com/historical-market-data/ (accessed: 29.03.2017).
Historiske priser i Hafslund Netts forsyningsområde. (2016). Available at: https://www.hafslundnett.no/kunde/historiske_priser_i_hafslund_netts_forsyningsomraade/12328 (accessed: 07.03.2017).
Holstad, M., Aanensen, T. & Henriksen, G. (2016). *Electricity, 2015*. Available at: https://www.ssb.no/en/energi-og-industri/statistikker/elektrisitet/aar (accessed: 01.05.2017).
Homer Energy. (2016). *HOMER® Pro Version 3.7 User Manual*. Available at: http://homerenergy.com/pdf/HOMER_v3.7%20manual_updated-08-11.pdf (accessed: 28.03.2017).
Inflation indicators. (2017). Available at: http://www.norges-bank.no/en/Statistics/Inflation/Inflation-indicators/ (accessed: 03.04.2017).
International Energy Agency. (2016). *Key world energy statistics*. Paris: OECD/IEA. Available at: http://www.iea.org/publications/freepublications/publication/key-world-energy-statistics.html (accessed: 01.05.2017).
Jung, N., Moula, M. E., Fang, T. T., Hamdy, M. & Lahdelma, R. (2016). Social acceptance of renewable energy technologies for buildings in the Helsinki Metropolitan Area of Finland. *Renewable Energy*, 99: 813-824.
Kipping, A. & Trømborg, E. (2016). Modeling and disaggregating hourly electricity consumption in Norwegian dwellings based on smart meter data. *Energy and Buildings*, 118: 350-369.
Kipping, A. (2017a). *Hourly electricity consumption for a household in Ås, 2016* (email to Vegard Bøe 13.02.2017).
Kipping, A. (2017b). *RE: Hourly electricity consumption for a household in Ås, 2016* (email to Vegard Bøe 13.02.2017).
Kipping, A. (2017c). *RE: Temperature used in modelled hourly electricity data* (email to Vegard Bøe 20.04.2017).
Kost, C., Mayer, J. N., Thomsen, J., Hartmann, N., Senkpiel, C., Philipps, S., Nold, S., Lude, S., Saad, N. & Schlegl, T. (2013). Levelized Cost of Electricity Renewable Energy Technologies. Freiburg, Germany: Frauenhofer Institut For Solar Energy Systems ISE. 48 pp.
Koussa, D. S. & Koussa, M. (2015). A feasibility and cost benefit prospection of grid connected hybrid power system (wind–photovoltaic) – Case study: An Algerian coastal site. *Renewable and Sustainable Energy Reviews*, 50: 628-642.
Kroken, S. (2017). *Timesdata fra metrologistasjonen på Søråsfeltet* (email to Vegard Bøe 06.02.2017).

Lambert, T., Gilman, P. & Lilienthal, P. (2006). Micropower system modeling with homer. In Farret, F. A. & Simões, M. G. (eds) *Integration of alternative sources of energy*, pp. 379-418. Hoboken, N.J: IEEE Press Wiley-Interscience.
Mahesh, A. & Sandhu, K. S. (2015). Hybrid wind/photovoltaic energy system developments: Critical review and findings. *Renewable & Sustainable Energy Reviews*, 52: 1135-1147.
Manwell, J. F., McGowan, J. G. & Rogers, A. L. (2010). *Wind Energy Explained: Theory, Design and Application*. 2nd ed. Hoboken: Wiley.
Masters, G. M. (2013). *Renewable and Efficient Electric Power Systems*. 2nd ed. Hoboken, NJ, USA: John Wiley & Sons, Inc. 690 pp.
Messenger, R. A. & Ventre, J. (2005). *Photovoltaic Systems Engineering*. 2nd ed. Florida: CRC Press LLC. 458 pp.
Multiconsult. (2013). *Kostnadsstudie, Solkraft i Norge 2013*: Enova SF. Available at: https://www.enova.no/download?objectPath=upload_images/9EF9602A2B454C008F472DF2A98F6737.pdf (accessed: 29.03.2017).
Om FAGKLIM. (2017). Available at: https://www.nmbu.no/fakultet/realtek/laboratorier/fagklim/om-fagklim (accessed: 27.02.2017).
Pérez-Arriaga, I., Knittel, C., Miller, R., Tabors, R., Bharatkumar, A., Luke, M., Birk, M., Burger, S., Rodilla, P., Pablo Chaves, J., et al. (2016). *Utility of the future*. Cambridge: Massachusetts Institute of Technology Energy Initiative. Available at: http://energy.mit.edu/research/utility-future-study/ (accessed: 12.05.2017).
Prisområder historisk (elspot). (2016). Available at: http://www.statnett.no/Kraftsystemet/Kraftmarkedet/Prisomrader-historisk-elspot/ (accessed: 29.03.2017).
Ramsdal, R. (2017). *Det er flere tak å ta av, vi har så vidt bare skrapt litt i overflaten*. Available at: https://www.tu.no/artikler/norsk-solkraftutbygging-naer-firedoblet-i-2016-vi-har-savidt-skrapt-i-overflaten/377031 (accessed: 24.04.2017).
Rapporter elsertifikater. (2017). Available at: http://necs.statnett.no/WebPartPages/AveragePricePage.aspx (accessed: 28.04.2017).
Saheb-Koussa, D., Koussa, M., Belhamel, M. & Haddadi, M. (2011). Economic and environmental analysis for grid-connected hybrid photovoltaic-wind power system in the arid region. *Energy Procedia*, 6: 361-370.
Sarker, S. (2016). Feasibility analysis of a renewable hybrid energy system with producer gas generator fulfilling remote household electricity demand in Southern Norway. *Renewable Energy*, 87 (1): 772-781.
SB 1300TL-10. (2017). Available at: http://www.solcellespesialisten.no/inverter-vekselretter/1-fase/sb-1300tl-10.html (accessed: 21.04.2017).
Sørgard, L., Reiten, E., Bjella, K., Nesheim, H., Svihus, O., Wiermyhr, K., Sepúlveda, C., Rudi, A. G., Jenssen, Å. & Harsem, S. E. (2014). *Et bedre organisert strømnett*. Rapport Olje- og energidepartementet. Oslo: Olje- og energidepartementet. Available at: https://www.regjeringen.no/globalassets/upload/oed/pdf_filer_2/rapport_et_bedre_organisert_stroemnett.pdf (accessed: 12.05.2017).
Sreeraj, E., Chatterjee, K. & Bandyopadhyay, S. (2010). Design of isolated renewable hybrid power systems. *Solar Energy*, 84 (7): 1124-1136.
Statistikk: Bruk av solstrøm i Norge. (2017). Available at: http://solenergi.no/statistikk/ (accessed: 10.05.2017).

Statnett. (2017). *Nettutviklingsplan 2017*. Nettutviklingsplan. Oslo: Statnett. Available at: http://www.statnett.no/Nettutvikling/Nettutviklingsplan-2017/ (accessed: 12.05.2017).
Türkay, B. & Telli, A. Y. (2011). An Economic Analysis of Grid-connected Hybrid Energy Systems. *Energy Sources, Part B: Economics, Planning, and Policy*, 6 (3): 228-241.
Våre betingelser for Nabostrøm™. (2017). Available at: https://www.otovo.no/nabostrom/betingelser (accessed: 09.03.2017).

Attachments

Attachment 1: Specification sheets for the PV-module IBC Polysol 250 VM.

Smart Systems
for Solar Power

IBC SOLAR

IBC EcoLine - For particulary stable output

IBC PolySol 240 VM, 245 VM, 250 VM

Solar modules made by polycrystalline silicon

Regardless of whether it is used on detached houses, the roofs of industrial properties or on open spaces, tried and tested IBC PolySol VM photovoltaic modules are suitable for any application requiring a high quality, efficiency and profitability. Continuous quality assurance and process audits during production guarantee a particularly long service life of the modules with a maximum of output, efficiency and reliability. Thanks to the antireflective coating on the front glass panels, these modules capture even more light to be more efficient and produce optimum yields.

Highlights

- 10-year product warranty*
- 25 years linear power warranty*
- Positive Power tolerance: -0/+5 Wp
- Highly effective with low-iron photovoltaic glass and anti-reflective coating (3.2mm)
- Sturdy hollow-chamber frame
- Tested according IEC 61215 for snow loads up to 5400 Pa (ca. 550 kg/m²)
- IEC 61730, application class A for system voltages up to 1000 V, protection class II
- Produced in facilities certified as per ISO 9001, ISO 14001 and OHSAS 18001
- Regular product/process/quality assurance audits in production
- Quality tested by IBC SOLAR in own laboratory with climate chambers and flasher with integrated electroluminescence measurement

CE

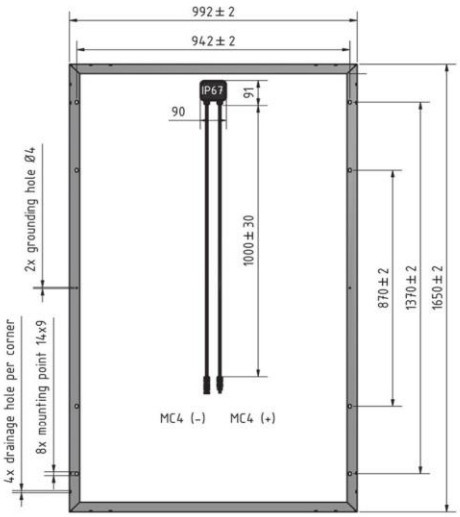

Progression of the power warranty

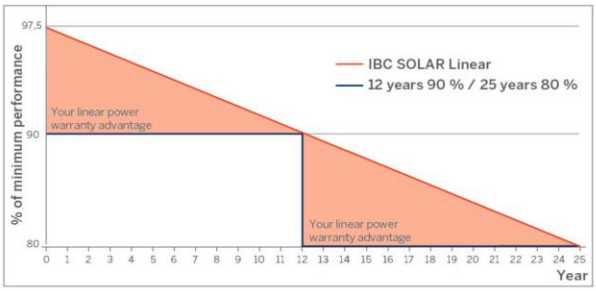

TECHNICAL DATA

IBC PolySol	240 VM	245 VM	250 VM
STC Power Pmax (Wp)	240	245	250
STC Nominal Voltage Umpp (V)	30.0	30.2	30.4
STC Nominal Current Impp (A)	8.01	8.12	8.23
STC Open circuit voltage Uoc (V)	37.2	37.4	37.6
STC Short circuit current Isc (A)	8.56	8.69	8.81
800 W/m² NOCT AM1.5 Power Pmax (Wp)	173.0	176.4	180.1
800 W/m² NOCT AM1.5 Nominal Voltage Umpp (V)	27.3	27.4	27.7
800 W/m² NOCT AM1.5 Open Circuit Voltage Uoc (V)	33.6	33.8	33.9
800 W/m² NOCT AM1.5 Short Circuit Current Isc (A)	6.91	6.99	7.07
Rel. efficiency reduction @ 200W/m² (%)	5	5	5
Tempcoeff Isc (%/°C)	+0.06	+0.06	+0.06
Tempcoeff Uoc (mV/°C)	-133.9	-134.6	-135.4
Tempcoeff Pmpp (%/°C)	-0.48	-0.48	-0.48
Module Efficiency (%)	14.7	15.0	15.3
NOCT (°C)	46	46	46
Max. System Voltage (V)	1000	1000	1000
Max. Reverse Current Ir (A)	20	20	20
Current value String fuse (A)	15	15	15
Fuse protection from parallel strings	4	4	4
Height (mm)	45	45	45
Weight (kg)	19.3	19.3	19.3
Article number	2204000001	2204000002	2204000003

2014-01-30

Presented by:

* The linear power warranty is only valid for installations within Europe and Japan. For further information, please refer to the corresponding product and power warranty in accordance with the version of the full warranty conditions received from your specialized IBC SOLAR partner at the time of installation. This warranty is valid only when the product is installed in accordance with the applicable installation instructions. Electrical values under standard test conditions: 1000W/m²; 25°C, AM1.5. 800 W/m², NOCT. Specifications according EN 60904-3 (STC). All datas according DIN EN 50380. Subject to modifications that represent progress.

Attachment 2: Specification sheets for the inverter SB1300TL-10.

Smart Systems
for Solar Power

IBC SOLAR

Powerful expertise

SMA SB 1300TL-10, SB 1600TL-10, SB 2100TL-10

Inverter

Its low weight, robust housing, and attractive efficiency of 96 percent make the Sunny Boys an ideal starter model. With its wide range of input voltage and input current, it is compatible with almost all common crystalline solar modules. And thanks to its three power classes, it is also suitable for smaller photovoltaic systems.

Highlights

- Ideal for small photovoltaic systems
- Maximum efficiency of 96%
- Convection cooling
- Integrated DC circuit breaker Electronic Solar Switch (ESS) (optinal)
- SUNCLIX DC connection system

TECHNICAL DATA

Sunny Boy	1300TL-10	1600TL-10	2100TL-10
Input			
DC-nominal power (W)	1400	1700	2200
Max. input current (A)	12	12	12
Max. input voltage(V)	600	600	600
Max. MPP-voltage (V)	480	480	480
Min. MPP-voltage (V)	115	155	200
Output			
Power factor (cos phi)	1	1	1
number of grid input phases	1	1	1
Min. AC frequency (Hz)	44	44	44
Max. AC frequency (Hz)	55	55	55
Min. AC grid voltage (V)	180	180	180
Max. AC grid voltage (V)	260	260	260
Degree of efficiency			
AC-nominal power (W)	1300	1600	1950
Max. efficiency (%)	96.0	96.0	96.0
Euro. efficiency (%)	94.3	95.0	95.2
Operating consumption in night mode (W)	0.1	0.1	0.1
Security			
Technology	TRANSFORMERLESS	TRANSFORMERLESS	TRANSFORMERLESS
Conditions			
Ambient temperature (°C)	-25 TO +60	-25 TO +60	-25 TO +60
Humidity (%)	0 TO 100	0 TO 100	0 TO 100
Equipment			
Type of DC-connector	SUNCLIX	SUNCLIX	SUNCLIX
DC switch	YES	YES	YES
Protection rating (IP)	65	65	65
Width (mm)	440	440	440
Height (mm)	339	339	339
Depth (mm)	214	214	214
Weight (kg)	16	16	16
Output cross section (mm^2)	2.5	2.5	2.5
Article number	**3000100261**	**3000100262**	**3000100263**

2014-01-28

Presented by:

* Product and power warranty in accordance with the version of the full warranty conditions received from your IBC SOLAR partner at the time of installation. This warranty is valid only when the relevant product is installed in accordance with the applicable installation instructions. Subject to modifications that represent progress.

IBC SOLAR AG | Am Hochgericht 10, 96231 Bad Staffelstein, Germany | Phone +49 (0) 9573 9224 0 | Fax +49 (0) 9573 - 92 24 111 | info@ibc-solar.com | www.ibc-solar.com

Attachment 3: Pages from the certification document of the wind turbine Avance R9000.

2. Power Curve

Table 1 and Table 2 show the power performance results at sea level air density for the Evance R9000.

BWEA Reference Power (Watts)	4711
Cut-in Wind Speed (m/s)	3
Maximum Power (Watts)	5254

TABLE 1 - BWEA DEFINITION RESULTS

Measured power curve							
Reference air density: 1.225kg/m³					Category A	Category B	Combined uncertainty
Bin no.	Hub height wind speed m/s	Power output Watts	C_p	No. of data sets 1 min. Avg.	Standard uncertainty s_i Watts	Standard uncertainty u_i Watts	Standard uncertainty u_{ci} Watts
1	0.59	9	0	38	0	18	18
2	1.00	5	0	69	1	18	18
3	1.53	-3	0	154	1	18	18
4	2.03	-4	0	294	0	18	18
5	2.50	-2	0	457	0	18	18
6	3.00	13	0.03	476	1	19	19
7	3.53	73	0.11	806	2	34	34
8	4.00	201	0.21	1160	3	72	72
9	4.51	385	0.29	1197	4	99	99
10	5.00	619	0.34	1319	5	129	129
11	5.50	864	0.36	1389	6	139	139
12	6.00	1174	0.37	1306	7	175	175
13	6.50	1508	0.38	1369	8	196	196
14	7.00	1894	0.38	1433	9	231	231
15	7.50	2271	0.37	1561	9	228	229
16	8.01	2710	0.36	1757	10	268	269
17	8.50	3150	0.35	1806	10	281	281
18	9.00	3523	0.33	1900	11	244	244
19	9.50	3918	0.31	1951	10	260	260
20	10.00	4244	0.29	1885	9	224	225
21	10.49	4496	0.27	1713	9	178	178
22	10.99	4711	0.24	1453	8	155	155
23	11.49	4834	0.22	1167	7	98	98
24	11.99	4929	0.20	964	7	80	80
25	12.48	4975	0.18	724	7	53	53
26	12.99	4971	0.16	508	10	41	42
27	13.49	4972	0.14	314	15	41	43
28	13.99	4947	0.12	238	23	45	50

3. Annual Energy Production

Table 3 gives the BWEA Reference Annual Energy for the Evance R9000. Table 4 shows the AEP estimations for hub height integer annual average wind speeds from 4m/s, up to the maximum wind speed for the turbine Class (i.e. 4, 5, 6, 7 and 8m/s for the Class II Evance R9000) at sea level air density.

BWEA Reference Annual Energy (kWh)	9170 (3 significant figures)

TABLE 3 - BWEA REFERENCE ANNUAL ENERGY

Estimated Annual Energy Production Reference Air Density: 1.225kg/m^3 Cut Out Wind Speed: No cut out wind speed but extrapolation taken up to 25 m/s					
Hub height annual average wind speed (Rayleigh) m/s	AEP-measured (measured power curve) kWh	Standard uncertainty in AEP kWh	Standard uncertainty in AEP %	AEP-extrapolated (extrapolated power curve) kWh	
4	4962	746	15	4962	COMPLETE
5	9164	1003	11	9167	COMPLETE
6	13605	1152	8	13653	COMPLETE
7	17586	1204	7	17877	COMPLETE
8	20654	1194	6	21582	COMPLETE

TABLE 4 - ESTIMATED ANNUAL ENERGY PRODUCTION AT SEA LEVEL AIR DENSITY, 1.225kg/m^3

Figure 2 shows the expected annual energy production for the Evance R9000 at various hub height wind speeds in graphical format.

29	14.49	4931	0.11	178	30	42	52
30	14.96	4965	0.10	113	39	51	64
31	15.49	5014	0.09	91	45	56	72
32	15.98	5079	0.09	63	40	69	80
33	16.47	5096	0.08	45	28	44	52
34	17.00	5073	0.07	28	49	45	66
35	17.42	5056	0.07	12	64	45	78
36	17.91	5072	0.06	6	58	44	73
37	18.40	5026	0.06	4	142	59	154
38	19.13	5123	0.05	1	0	75	75

TABLE 2 - POWER PERFORMANCE RESULTS AT SEA LEVEL AIR DENSITY, 1.225kg/m³

Figure 1 shows the Evance R9000 power curve normalised to sea level air density, 1.225kg/m³. The combined standard uncertainties of the results are indicated on the graph by the vertical error bars.

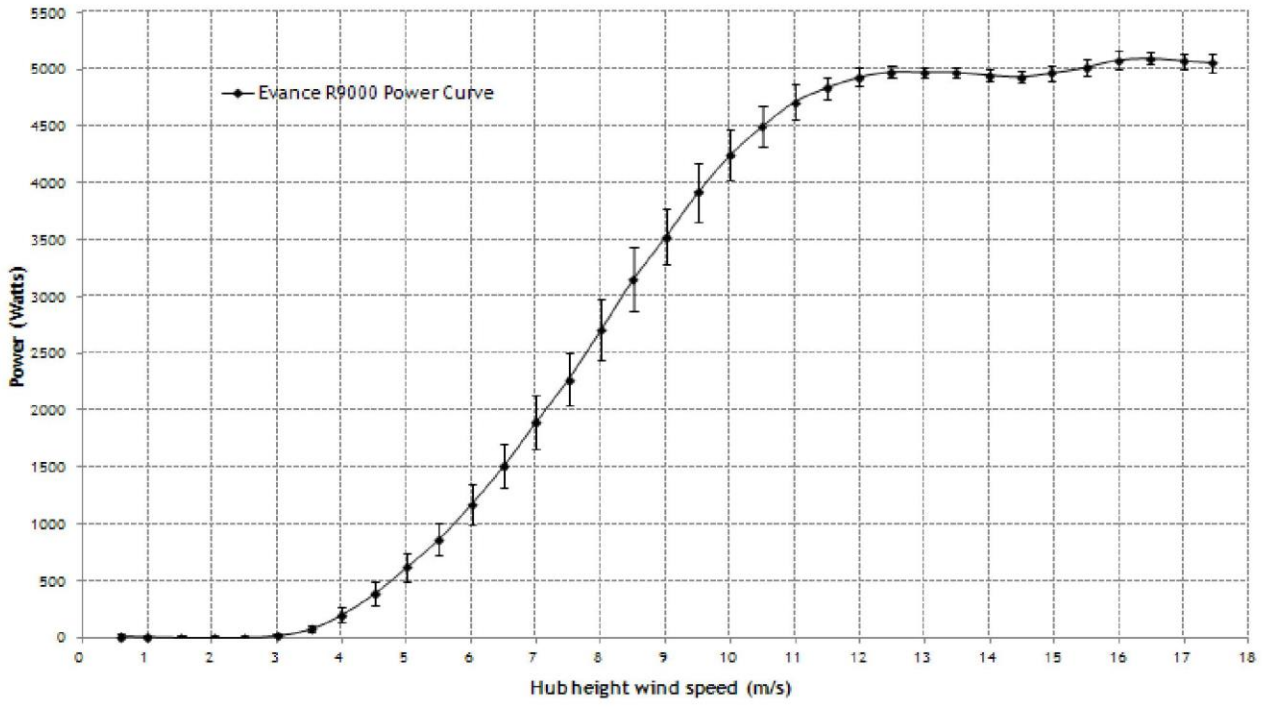

FIGURE 1 - POWER CURVE AND COMBINED STANDARD UNCERTAINTY AT SEA LEVEL AIR DENSITY, 1.225kg/m³

Norges miljø- og biovitenskapelig universitet
Noregs miljø- og biovitskapelege universitet
Norwegian University of Life Sciences

Postboks 5003
NO-1432 Ås
Norway